UNIVERSITY
OF ALASKA

COLLEGE
ALASKA

UAG - R134

RADIO-STAR VISIBILITY FADES OBSERVED IN THE AURORAL ZONE

by

Edward J. Fremouw

Contract No. NAS5 - 1413

Aberrations of Radio Signals Traversing
the Auroral Ionosphere

SCIENTIFIC REPORT NO. 1

PART 1

April 1963

Prepared for

National Aeronautics and Space Administration
Goddard Space Flight Center

GEOPHYSICAL INSTITUTE

of the

UNIVERSITY OF ALASKA

RADIO-STAR VISIBILITY FADES OBSERVED IN THE AURORAL ZONE

by

Edward J. Fremouw

Scientific Report No. 1
Part 1

Contract No. NAS5-1413

Aberrations of Radio Signals Traversing the Auroral Ionosphere

Prepared for

NATIONAL AERONAUTICS AND SPACE ADMINISTRATION
GODDARD SPACE FLIGHT CENTER

Principal Investigator:

Leif Owren

Approved by:

C. T. Elvey
Director

April 1963

ABSTRACT

The operation of a phase-switch interferometer is analysed to show that reductions in output may be interpreted as reductions in correlation between signals arriving at the two antennas. Such reductions, therefore, constitute decreases in the visibility of the source under observation. Visibility fades of the radio stars Cygnus A and Cassiopeia A, observed on 223 megacycles in the auroral zone during one year of maximum sunspot activity, are analysed empirically. Fade-occurrence distributions in time and space are presented and comparisons with certain other geophysical phenomena are discussed. Fades observed on 456 megacycles during one month are compared with those observed on 223 megacycles.

The visibility fades appear to be caused by scattering irregularities whose geographical distribution peaks near the maximum of the visual auroral zone. There is evidence of contributions from both the E-layer and F-layer. Primary occurrence maxima appear in autumn and at magnetic midnight.

TABLE OF CONTENTS

LIST OF FIGURES

I. INTRODUCTION

Since the first observation of radio stars by Hey, Parsons, and Phillips (1946), it has been consistently noted that their signals are not of constant intensity when observed at the earth's surface. Indeed, it was the fluctuation of such signals which led Hey, Parsons, and Phillips to postulate the discrete nature of the sources. Smith, Little, and Lovell (1950) suggested a terrestrial origin of the fluctuations rather than an intrinsic one as assumed by the discoverers. The terrestrial origin of the fluctuations was verified repeatedly by workers in several countries and the term "scintillation" has been applied to them quite generally. Extensive investigation of radio-star scintillations has now been carried out at both middle and high latitudes, notably at Cambridge and Manchester, England; in Australia; and at College, Alaska. The middle-latitude studies have been summarized by Little, Rayton, and Roof (1956), and the early Alaskan work was reported by Little, Reid, Stiltner, and Merritt (1962).

The above-mentioned and related observations of radio-star scintillation led to theoretical search for a model to explain its production. The model now generally accepted is that of a diffracting layer of irregular ion concentration in the terrestrial ionosphere. Notable theoretical papers concerning the effects of such a model on radio-star-like signals are those of Booker, Ratcliffe, and Shinn (1950),

Hewish (1951) and Fejer (1953). Ratcliffe (1956) has written a comprehensive summary of the theory. Further theoretical work has been published by Booker (1958) along with additional discussion of observational results. The above-mentioned papers do not at all represent an exhaustive list of publications on the subject but do serve to outline its development.

Among the techniques used for observation of radio stars have been those of radio interferometry. Solar radio astronomy in Australia had made use of signal reflection from the sea to provide an interferometer requiring only one antenna (McCready, Pawsey, and Payne-Scott, 1947), and Bolton and Stanley (1948) used the device for early radio-star work. Scintillation studies, using the same instrument (the "cliff interferometer"), were carried out by Bolton, Slee, and Stanley (1953). Subsequently, interferometers using two or more antennas have come into use, radio-star scintillation being studied on a variety of two-antenna (or "twin-wave") instruments.

Scintillation studies at College have employed three types of twin-wave interferometer: total-power, phase-switch, and phase-sweep. It was on phase-switch and phase-sweep interferometers operating on 223 MC and 456 MC at College that radio-star visibility fades - the subject of this paper - were first observed (Little, Merritt, Stiltner, and Cognard, 1957). The fades, termed "long-duration fades" by the discoverers, appeared on the phase-switch records as partial or complete disappearances of the quasi-sinusoidal interference

pattern of the star. On the phase-sweep records they appeared as depressions in the ordinate of the record, averaged over a period of several scintillations. Reproductions of the originally reported fade records appear in figures 1 and 2. Fade durations from several minutes to over an hour were observed. The discoverers interpreted the fades in terms of irregularities which subtended a solid angle less than that of the source, thereby causing different parts of the source to scintillate independently (Little, Reid, Stiltner, and Merritt, 1962).

Apparently little or no investigation of visibility fades, beyond inspection of certain other geophysical records obtained during a particularly long fade (Little, Merritt, Stiltner, and Cognard, 1957), was carried out in the auroral zone between their discovery and 1962. Owren (1962a) has written a review of radio-wave scattering theory as applicable to radio-star and satellite scintillation questions and has extended the theory to describe the phenomenon of radio-star visibility fades in terms of thick-layer multiple scattering. He has shown that for such a scattering mechanism, visibility fades may be expected even for point sources, relaxing the requirement supposed by Little, Reid, Stiltner, and Merritt (1962) that the source must subtend a greater angle than the scattering irregularities. The latter conclusion apparently resulted from considering only simple thin-layer scattering.

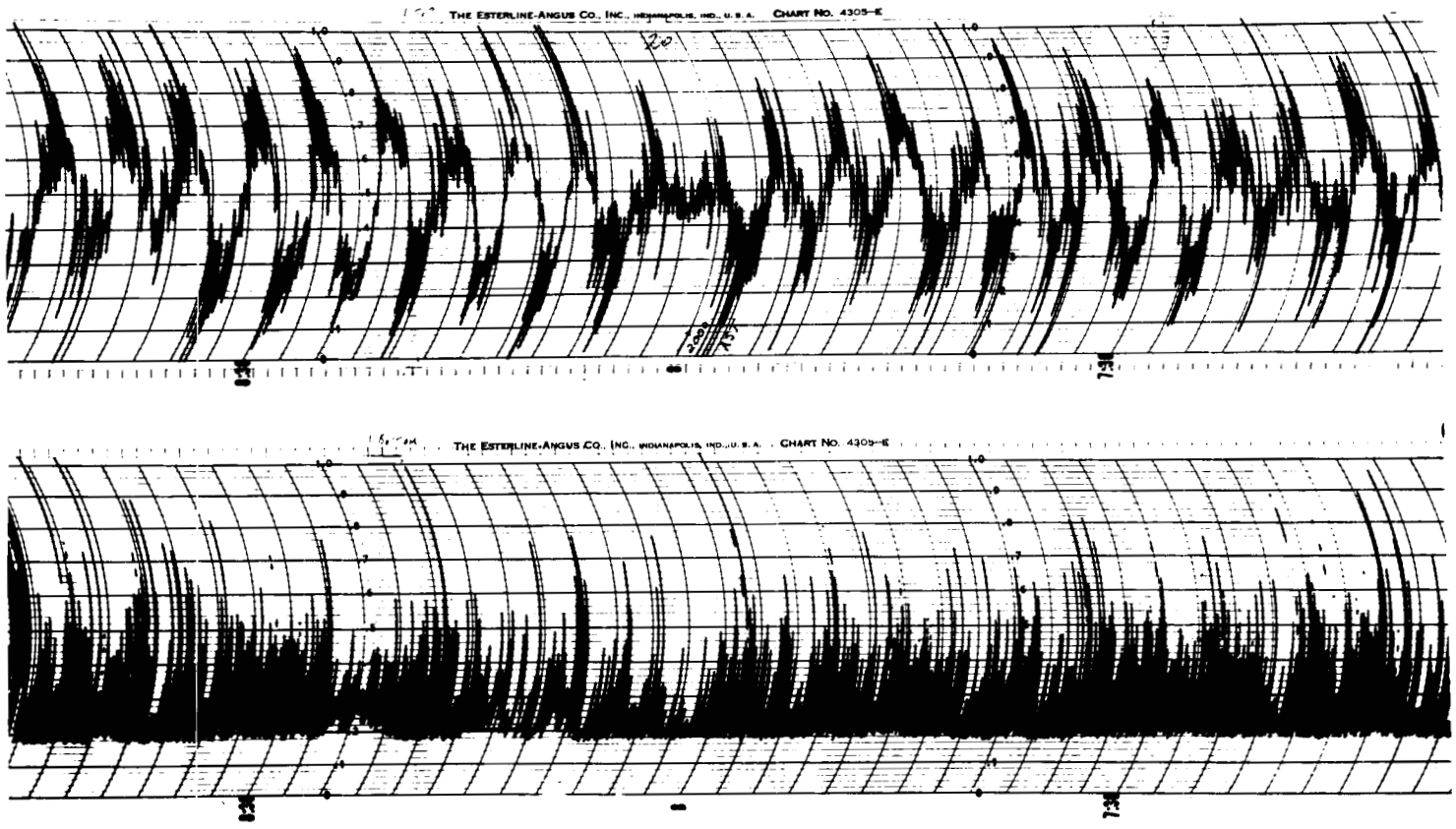

Fig. 1. Visibility Fade Observed by Little, et al, on Phase-Switch Interferometer.

Fig. 2. Simultaneous Phase-Sweep Record Obtained by Little, et al.

The empirical work reported in this paper has been carried out in conjunction with the theoretical work of Owren, mentioned above. Its purpose is to present the observed characteristics of auroral-zone visibility fades. The paper is primarily concerned with the statistics of fade occurrence - i.e., their distributions in time and space. Some investigation has been carried out, also, of ionospheric and geomagnetic conditions during fades and of the frequency dependence of fade occurrence, toward the end of providing data for further theoretical studies of ionospheric irregularities in the auroral zone.

It is to be noted that, while experimental investigation of radio-star visibility fades in the auroral zone has been extremely limited since their discovery, relatively elaborate studies have been carried out at lower latitude (Nichols, 1960; Flood, 1962). Recently, Moorcroft (1963) has reported on work carried out at Saskatoon.

II. INSTRUMENTATION

The records used in this study were those gathered by Little and his co-workers during the time of their original observations of radio-star visibility fades. Little's group operated total-power, phase-switch, and phase-sweep interferometers on frequencies of 223 MC and 456 MC. While fades were originally reported on both the phase-switch and phase-sweep devices, it was decided to use records from only one kind of interferometer for this study in order to keep the total number of data to be handled within manageable bounds. It was found that, of the four instruments which apparently were capable of recording fades, the 456 MC phase-sweep interferometer had produced the least complete set of data during the period of operation. It was decided, therefore, to use the phase-switch records rather than the phase-sweep.

As pointed out by Flood (1962), "There appears to be some confusion about the relationship between the input and the output of phase swept and phase switched interferometers." In particular, it is evident in some of the literature that the operational differences between the two devices are sometimes overlooked or confused. Since a thorough understanding of the operations carried out by an interferometer on its input signal is prerequisite to an understanding of visibility fades which may be observed with it, a mathematical presentation of those operations for the phase-switch

interferometer is given below. The first part of this presentation parallels that given by Flood (1962) for the phase-swept case although it is meant to be somewhat more general. It is hoped that the existence of two independent but parallel derivations for the two kinds of instruments, each in a notation appropriate to visibility-fade application, will be useful to further understanding of the phenomenon.

Consider a phase-switch interferometer with its two antennas situated in a radio-star wave-field. The voltage output of each antenna consists of the phasor sum of all the components of the wave's angular and frequency spectra plus similar components from galactic noise and other sources, integrated over the field of view and passband of the antenna. Considering a single angular component,[1] the output of the antennas may be written as follows:

$$e_1(t) = \int E_1(f)\, e^{j\omega t}\, df \qquad (1)$$

$$e_2(t) = \int E_2(f)\, e^{\left[j\omega t + j\theta(f) + j\phi(f)\right]} df \qquad (2)$$

where the limits of integration are set by the effective passband (assumed rectangular) of the antennas. $\theta(f)$ represents a phase difference between the two signals determined by the arrival direction of the angular component under discussion, and $\phi(f)$ represents an additional phase difference due to any other cause.

---

[1] This restriction will be discussed later and removed for the case of random phases in the angular spectrum.

In the case of the instruments used in this study, the signals $e_1(t)$ and $e_2(t)$ are amplified in radio-frequency amplifiers, their frequencies converted, and they are again amplified in separate intermediate-frequency amplifiers. With all circuits assumed ideal (rectangular passbands and no phase shift introduced) and with gains normalized to unity, equations (1) and (2) still represent the signals after the above-mentioned operations have been performed except that the center frequency and the limits of integration are set now by the i-f passband.

Next, the signal from one of the antennas, $e_2(t)$ say, is passed through the phase switch. The result is an additional phase term, such that $e_2(t)$ becomes

$$e_2'(t) = e^{j\psi(t)} \int E_2(f)\, e^{\left[j\omega t + j\theta(f) + j\phi(f)\right]} df \qquad (3)$$

where $\psi(t)$ is a periodic time function. In general, ψ may be a function of frequency, f, as well as of time, especially in an interferometer using a switching harness type of phase switch as is the case with the instruments used in this study. The frequency dependence of ψ, however, is comparable with that of phase shifts inherent in other circuits, which already have been assumed negligible. A simple calculation shows that the change in magnitude of ψ across typical i-f bandwidths is of the order of one electrical degree. Accordingly, ψ may be considered frequency independent for present purposes and has been placed outside the integral in equation (3). It is to be remembered, also, that θ, E_1, E_2, and ϕ,

as well as ψ, may be time-varying. Indeed, the term "scintillations" refers specifically to the fluctuations of the latter three of these quantities, and θ varies due to the earth's rotation. The notation $\psi(t)$ has been used to retain attention on the fact that ψ, thus far, has not been explicitly defined.

After the phase-switching operation, the signals from the two antennas are added and their sum applied to another intermediate-frequency amplifier, which in the College instruments actually determines the i-f bandwidth. $e_1(t)$ and $e_2'(t)$ are passed unaltered, except for the limits of integration, so the output of this main i-f amplifier may be written as

$$e_3(t) = \int E_1(f)\, e^{j\omega t} df + e^{j\psi(t)} \int E_2(f)\, e^{\left[j\omega t + j\theta(f) + j\phi(f)\right]} df \qquad (4)$$

The output of the main i-f amplifier is applied immediately to a second detector which approximates to a square-law device. Assuming square-law operation, the second-detector output may be written as

$$\begin{aligned} e_4(t) = {} & \iint E_1(f)E_1(f+f')e^{j\omega t}e^{-j(\omega+\omega')t}\,df'df \\ & + \iint E_2(f)E_2(f+f')e^{\left[j\omega t+\theta(f)+\phi(f)\right]}e^{-j\left[(\omega+\omega')t+\theta(f+f')+\phi(f+f')\right]}\,df'df \\ & + e^{-j\psi(t)} \iint E_1(f)E_2(f+f')e^{j\omega t}e^{-j\left[(\omega+\omega')t+\theta(f+f')+\phi(f+f')\right]}\,df'df \\ & + e^{j\psi(t)} \iint E_2(f)E_1(f+f')e^{j\left[\omega t+\theta(f)+\phi(f)\right]}e^{-j(\omega+\omega')t}\,df'df \end{aligned} \qquad (5)$$

Equation (5) requires discussion in detail. It ensues directly from complex squaring of equation (4), with all cross-terms between frequency components taken into account. The inner integrals are to be taken over the variable, f',

from $-\frac{\Delta f'}{2}$ to $+\frac{\Delta f'}{2}$, where $\Delta f'$ represents the i-f bandwidth. The outer integrals are to be taken over the variable, f, from $f_o - \frac{\Delta f}{2}$ to $f_o + \frac{\Delta f}{2}$, where f_o is the center frequency in the radio-frequency passband and Δf is here used to represent the i-f bandwidth and is numerically equal to $\Delta f'$. Thus, f represents radio-frequency components and f' represents increments of frequency in the r-f spectrum. The variable, ω, of course, represents components of angular frequency in the i-f spectrum and differs from f only by a numerical constant (the local-oscillator frequency) and a multiplying factor (2π). ω' represents increments of angular frequency measured from ω.

Equation (5) may be simplified greatly in the case of interferometric studies of radio-star scintillation. The simplification results from the fact that the signal variations (scintillations) under study have durations many times longer than the reciprocal of the i-f bandwidths used. For such relatively slow variations, only a very small band of frequencies (compared with the i-f bandwidth) centered around each component in the i-f spectrum contributes appreciably to the Fourier spectrum produced by complex-amplitude variations of that component. It is this and only this very small band which contains frequencies whose relative phase will remain essentially constant during the time of a single variation.[1]

---

[1] This is the frequency-domain analogue of the time-domain statement made by Born and Wolf (1959) in the next-to-last sentence of the second paragraph of their Chapter X.

The i-f spectrum, therefore, is made up of a large number of relatively very narrow bands of "correlated" frequency components; the correlation between components in different bands is essentially zero. Accordingly, the inner integral in each of the four terms of equation (5) reduces to an integral taken over essentially infintesimal bandwidth, with the result that equation (5) becomes

$$e_4(t) = \int E_1^2(f)df + \int E_2^2(f)df + e^{-j\psi(t)}\int E_1(f)E_2(f)e^{-j\left[\theta(f)+\phi(f)\right]}df + e^{j\psi(t)}\int E_1(f)E_2(f)e^{j\left[\theta(f)+\phi(f)\right]}df \qquad (6)$$

The reduction of equation (5) to equation (6) is tantamount to saying that the i-f spectrum in the interferometer may be treated as uncorrelated noise and it is a necessary and sufficient argument to justify the statement by Flood (1962) that "due account of the bandwidth of the interferometer can be taken --- (by summing) --- the powers at each frequency in the pass band." Further, with the above result achieved for integration over the frequency spectrum while considering only one component of the angular spectrum, it would be possible now to start from the beginning of the development, integrating instead over the angular spectrum and considering only one component of the frequency spectrum. Exactly the same reduction of equation (5) to equation (6) would ensue provided that the phases in the angular spectrum could be taken as random. The assumption of random phases in the angular spectrum is certainly valid for signal components

coming from the galactic noise background, and it is commonly adopted in the case of scattered radio-star signals as well, (e.g., see Ratcliffe, 1956.) With both the frequency and angular spectra taken as uncorrelated within themselves, there is no reason to suspect correlation between signal components with different frequency as well as different angle. Hence, a fully general development, including integration over both frequency and angle, would also result in an expression of the form of equation (6) (except that the single integral would be replaced by a double integral), and a statement analagous to Flood's, above, could be made to the effect that "due account of the bandwidth of the interferometer and of the angular spectrum of the signal can be taken by summing the powers at each frequency in the passband and at each angle in the angular spectrum." The present analysis may be continued, therefore, on the basis of a single angular component, for the assumed case of random phases. It would be permissible, also, to carry on from here on the basis of a single frequency component, but the integral form of equation (6) will be retained for consistency.

It is now necessary to consider the explicit nature of $\psi(t)$. In the case of the phase-sweep interferometer, $\psi(t)$ is a linear function, producing a constantly advancing phase term in the interferometer equations. In the case of the phase-switch interferometer, however, $\psi(t)$ is more complicated; it is a square wave of base zero, amplitude π, and

frequency f_s. Accordingly, it may be written as the following Fourier series:

$$\psi(t) = \frac{\pi}{2} - 2\cos\omega_s t - \frac{2}{3}\cos 3\omega_s t + - - -$$
$$+ (-1)^{\frac{m-1}{2}}\frac{2}{m}\cos m\omega_s t + - - - \qquad m = 1,3,5, - - - \tag{7}$$

where $\omega_s = 2\pi f_s$. Now, equation (6) resulted from the action of the square-law detector on the i-f signal, $e_3(t)$, described by equation (4). In equation (4), $\psi(t)$ may be viewed as a phase modulation imposed upon the carrier wave of angular frequency, ω, so that the effect of the phase switch upon the i-f spectrum is to introduce sidebands displaced from each i-f frequency by each of the component frequencies of equation (7) and all harmonics thereof, plus corresponding sum and difference frequencies. Thus,

$$e^{j\left[\omega t+\psi(t)-\frac{\pi}{2}\right]} = \left\{\prod_{\substack{m=1\\ m\ \text{odd}}}^{\infty} J_0\left(\frac{2}{m}\right)\right\}\cos\omega t$$
$$+ \sum_{\substack{n=1\\ n\ \text{odd}}}^{\infty}(-1)^{\frac{n-1}{2}}\left\{\prod_{\substack{m=1\\ m\ \text{odd}}}^{\infty}(-1)^{\frac{m-1}{2}}J_n\left(\frac{2}{m}\right)\right\}\left\{\sin\sum_{\substack{m=1\\ m\ \text{odd}}}^{\infty}(\omega-nm\omega_s)t - \sin\sum_{\substack{m=1\\ m\ \text{odd}}}^{\infty}(\omega+nm\omega_s)t\right\}$$
$$+ \sum_{\substack{n=1\\ n\ \text{even}}}^{\infty}(-1)^{\frac{n}{2}}\left\{\prod_{\substack{m=1\\ m\ \text{odd}}}^{\infty}J_n\left(\frac{2}{m}\right)\right\}\left\{\cos\sum_{\substack{m=1\\ m\ \text{odd}}}^{\infty}(\omega-nm\omega_s)t + \cos\sum_{\substack{m=1\\ m\ \text{odd}}}^{\infty}(\omega+nm\omega_s)t\right\} \tag{8}$$

where the J_n's represent Bessel functions of the first kind and order n. The action of the square-law detector is such

that the first term on the right of equation (8) is lost. The other terms are implicit in the last two terms of equation (6) with ω absent from the arguments and with $\frac{\pi}{2}$, which appears on the left side of equation (8) for convenience, added to the arguments.

The signal represented by equation (6), which implicitly includes the information of equation (8) as discussed above, is passed through either a video or audio amplifier whose center frequency is that of the phase switch (i.e., the fundamental frequency, f_s, of $\psi(t)$). The bandwidth of this amplifier varies among instruments currently in use. Whatever the bandwidth of the switch-frequency amplifier, its function is to provide amplification at the switch frequency, and the audio-frequency bandwidth of the interferometer is ultimately limited by the synchronous detector which follows the switch-frequency amplifier.[1] Typically, the bandwidth of the synchronous detector is of the order of a cycle per second, so only the fundamental switch-frequency terms of equation (8) contribute appreciably to the interferometer output.[2] The useful input to the synchronous detector, therefore, may be expressed be rewriting equation (6) in a form which

---

[1] An advantage in signal-to-noise ratio at the input to the synchronous detector is gained from narrow bandwidth of the switch-frequency amplifier.

[2] Herein, of course, lies the basis for the phase-switch interferometer's great sensitivity to discrete sources since the synchronous detector refuses to pass the vast majority of background sky noise and receiver noise.

explicitly contains the ω_s terms of equation (8). The first two terms of equation (6) are dc terms (or quasi-dc if the variations in E_1 and E_2 are recalled) and are lost in the switch-frequency amplifier. The last two terms reduce to

$$e_5(t) = \int E_1(f)E_2(f)\left\{\sin\left[\omega_s t - \frac{\pi}{2} - \theta(f) - \phi(f)\right] - \sin\left[\omega_s t + \frac{\pi}{2} + \theta(f) + \phi(f)\right]\right\} df \qquad (9)$$

where constants have been normalized along with circuit gains. Equation (9) may be manipulated as follows:

$$e_5(t) = -\int E_1(f)E_2(f)\left\{\cos\left[\omega_s t - \theta(f) - \phi(f)\right] + \cos\left[\omega_s t + \theta(f) + \phi(f)\right]\right\} df$$

$$e_5(t) = -\int E_1(f)E_2(f)\left\{\cos\left[\theta(f) + \phi(f)\right] \cos \omega_s t\right\} df \qquad (10)$$

The integrand of equation (10) is clearly a wave at switch frequency, amplitude modulated by the cosine of $\left[\theta(f)+\phi(f)\right]$. (The corresponding equation in an analysis of a phase-sweep interferometer would be a wave at switch frequency, phase modulated by the cosine of $\left[\theta(f)+\phi(f)\right]$; this difference is of fundamental importance to application of the two types of instruments.)

Besides sharply limiting the audio passband to a few cycles either side of the switch frequency, the synchronous

detector rectifies the signal of equation (10) and passes the result to a dc amplifier whose output may be written as[1]

$$e_6(t) = \iint E_1(f,t)E_2(f,t)\cos\left[\theta(f,t) + \phi(f,t)\right] df\, dt \tag{11}$$

In (11), the limits of time integration are set by the output time-constant of the interferometer, which in the case of the College instruments, is fixed at the input to the dc amplifier. The variation of θ with radio-star hour-angle is such that, for E_1, E_2, and ϕ constant, the dc amplifier output to the pen recorder, which follows, is a quasi-sinusoidal function of time. Changes in (E_1E_2) and ϕ, of course, result in departures from the quasi-sinusoidal trace and represent amplitude and phase scintillations, respectively.

Consider, for a moment, what the dc amplifier output would be with the dc terms of equation (6) restored:

$$\begin{aligned} e_6'(t) = &\iint E_1^2(f,t)\,df\,dt + \iint E_2^2(f,t)\,df\,dt \\ &+ \iint E_1(f,t)E_2(f,t)\cos\left[\theta(f,t)+\phi(f,t)\right] df\,dt \end{aligned} \tag{12}$$

Rewriting equation (12) in complex notation results in

$$\begin{aligned} e_6'(t) = &\iint E_1^2(f,t)\,df\,dt + \iint E_2^2(f,t)\,df\,dt \\ &+ \iint E_1(f,t)E_2(f,t)e^{j\left[\theta(f,t)+\phi(f,t)\right]} df\,dt \end{aligned}$$

---

[1] A negative sign has been absorbed into the constants in equation (11); the sign is irrelevant to the results and in practice can be chosen arbitrarily by reversing the phase of the synchronous detector's reference signal.

or
$$e_6'(t) = \iint E_1^2(f,t)\,df\,dt + \iint E_2^2(f,t)\,df\,dt + \iint \underline{E}_1^*(f,t)\underline{E}_2(f,t)e^{j\theta(f,t)}\,df\,dt \qquad (13)$$

where $\underline{E}_1$ and $\underline{E}_2$ are complex amplitudes. Further, consider contributions from all components of the angular spectrum of the wave-field as discussed beneath equation (6). Equation (13) then becomes

$$e_6'(t) = \iiint E_1^2(f,\sigma,t)\,df\,d\sigma\,dt + \iiint E_2^2(f,\sigma,t)\,df\,d\sigma\,dt + \iiint \underline{E}_1^*(f,\sigma,t)\underline{E}_2(f,\sigma,t)e^{j\theta(f,\sigma,t)}\,df\,d\sigma\,dt \qquad (14)$$

where σ represents the angle of arrival of signal components. The integrand of the third term on the right of (14), aside from the phase delay, θ[1], is the correlation function of the signals arriving at the two antennas. Further, comparison with equations (12) and (11) shows that this term is just the output of the phase-switch interferometer. Reductions in the interferometer output, then, represent reductions in the correlation function of the received signal.

The limits of the angular integration introduced above were not discussed in connection with equation (6); it is now necessary to do so. Had the present development been carried out in terms of an angular spectrum instead of a single component, the limits of angular integration would have been set, at the outset, by the antenna beamwidths. Due

---

[1] $\theta(f)$ is related to the τ of Born and Wolf (1959), section 10.3.1 by $\theta(f) = 2\pi f\tau$.

to the dependence of θ on σ, however, signal components from sources of appreciable angular extent cancel out of the third term of equation (14). For the case of a single discrete source[2], therefore, the output of a phase-switch interferometer may be written as

$$e_6(t) = \int_0^{\tau} \int_{\sigma_o-\Delta\sigma/2}^{\sigma_o+\Delta\sigma/2} \int_{f_o-\Delta f/2}^{f_o+\Delta f/2} \underline{E}_1^*(f,\sigma,t)\underline{E}_2(f,\sigma,t)e^{j\theta(f,\sigma,t)}\,df\,d\sigma\,dt \qquad (15)$$

where f_o is the center frequency in the r-f passband, Δf is the i-f bandwidth, σ_o represents the direction of the source, $\Delta\sigma$ is the apparent angular diameter of the source, and τ is the output time constant.

Equation (15) shows that the output of a phase-switch interferometer is proportional to the correlation existing between the signals arriving at the two antennas, integrated over i-f bandwidth, output time constant, and apparent angular extent of the discrete source under track. It is, therefore, a direct measure of the spatial autocorrelation of the source's wave-field at the earth's surface, for the antenna spacing employed.

---

[2] Source confusion is not a common problem in ionospheric radio astronomy since only the strongest discrete sources usually are used.

III. DATA ANALYSIS TECHNIQUES

A. Reduction of Interferometer Data

One year's records from a phase-switch interferometer operating on 223 MC with an east-west baseline of 91.44 meters (68.8 wavelengths) were inspected for visibility fades. The records used had been collected at College during the period of 1 November 1957, through 31 October 1958. This period fell completely within the International Geophysical Year, thus corresponding to a period of maximum solar activity and acceptably consistent data. The entire year's records were inspected grossly for possible visibility fades. The possible fades then were inspected more closely and scaled according to the following scheme.

First the times of onset and ending of an apparent fade were marked on the record margin. In a large majority of cases, these times were quite readily identifiable to within one minute. Onset and end having been established, individual scintillations were averaged out visually to reveal any residual radio-star interference pattern existing during the period in question. Next, the maxima and minima of the nearest undisturbed interference pattern were marked to establish normal levels under current operating conditions.

The character of the interference pattern having been determined both during the possible fade and during a shortly preceding or following period, the visibility of the radio star during the suspected fade was calculated. This was done

simply by taking the ratio of the pattern amplitude during the time in question to that during the normal period. The technique is illustrated in figure 3, which is an idealization of a fade record.

The top and bottom horizontal lines in figure 3 mark the maximum and minimum of the undisturbed radio-star pattern, the latter corresponding to zero resultant star power. The broken horizontal line corresponds to the level of the d.c. terms appearing in equation (14) of Section II, which are rejected by the phase-switching action of the interferometer. Starting approximately at time T_o the record does not rise, at maximum, to the top line nor fall, at minimum, to the bottom line. Instead, it rises only to the level marked P_{max} and drops only to the level marked P_{min}. The decrease in amplitude of the quasi-sinusoidal trace, noted from time T_o on, represents a decrease in the visibility of the radio star. Visibility, in fact, can be defined as $(P_{max} - P_{min})/(P_{max} + P_{min})$, so it is given by the ratio B/A, where B is the reduced amplitude and A the normal amplitude of the trace.[1]

In practice, the reduced amplitude seldom remains constant for more than one fringe of the interference pattern.

---

[1] From inspection of figure 3, it is clear that

$$P_{max} = P_{mean} + B,\quad P_{min} = P_{mean} - B,\quad \text{and}\quad P_{mean} = A.$$

It follows that

$$\text{Visibility} = 2B/2P_{mean}$$

or

$$\text{Visibility} = B/A$$

The value used for B in calculating visibility, therefore, was often an average of two or more chart measurements. Further, the interference pattern observed during and near visibility reductions is nearly always accompanied by considerable scintillation; the idealized pattern of figure 3 is representative only of an already averaged record and not of a typical unprocessed record. An actual record with scaling notations is shown in figure 4.

Once radio-star visibility was calculated during a suspected fade and the duration established, it was necessary to decide whether or not to record the event as a visibility fade. Criteria could be established quite arbitrarily since visibilities of all values from zero to unity were observed with a great variety of durations. This does not imply that it is difficult to distinguish periods of reduced visibility; it means, however, that varying degrees of disturbed conditions can and do produce varying amounts and durations of visibility reduction. In order to perform statistical studies of radio-star seeing conditions, therefore, it was convenient to set criteria for demarking "disturbed" conditions from "normal" conditions. Such demarkation led to the term, "visibility fade". For purposes of this study, visibility fades were defined as reductions in average visibility to 0.5 or less for a duration of three minutes or more. These criteria resulted in a meaningful statistical sample of fades while keeping the total number within the limits of manageability.

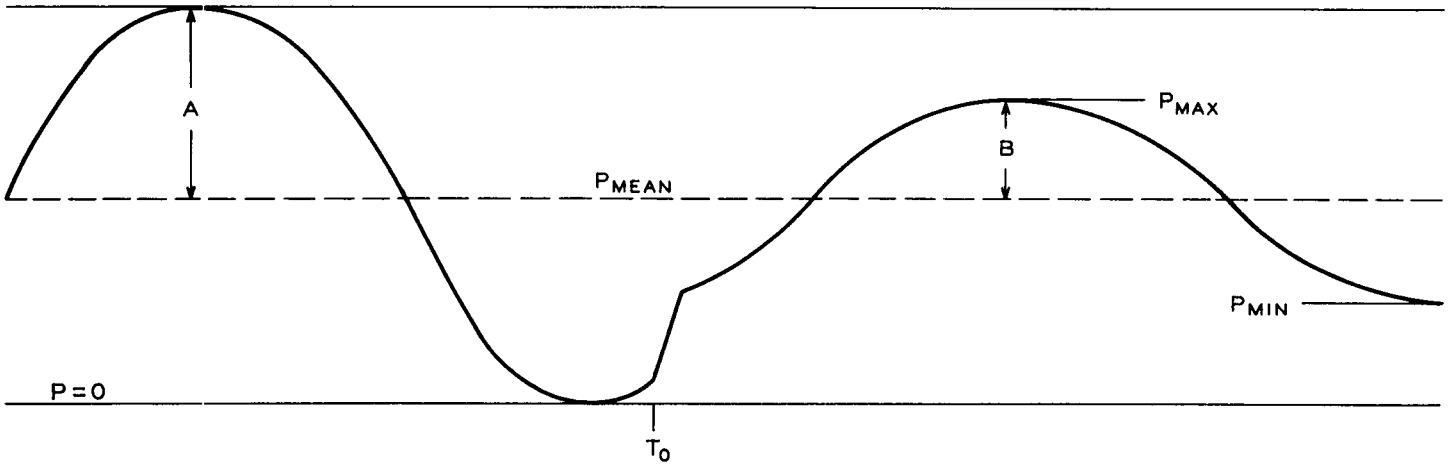

Fig. 3. Visibility-Fade Scaling Parameters.

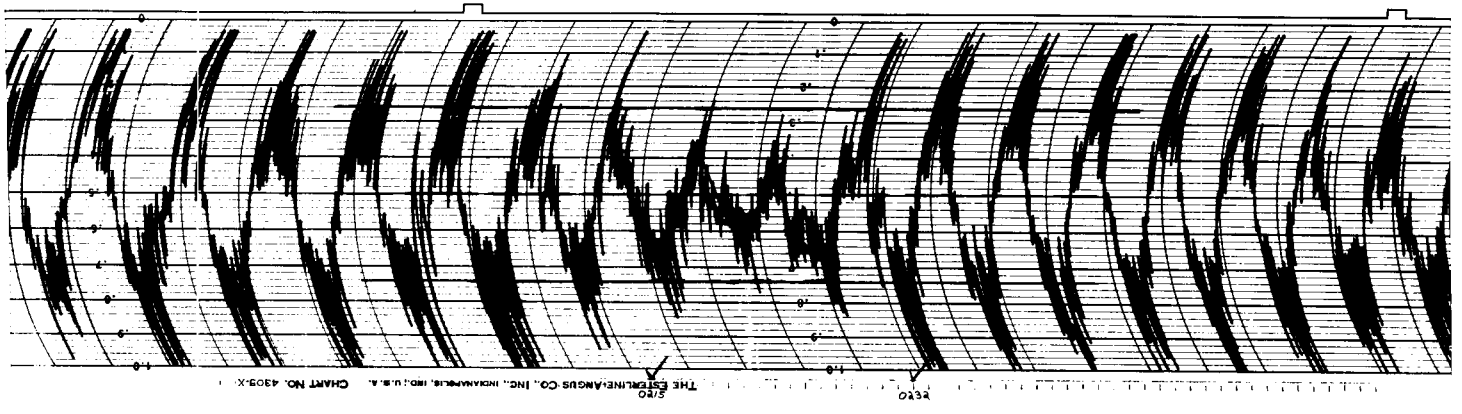

Fig. 4. Fade Record after Scaling.

It is to be noted that the duration criterion used for defining visibility fades resulted in the recording of many fades lasting less than one complete fringe of the interference pattern.[1] In such instances, the scaling technique described above was altered to include extrapolation of the smoothed interference trace from the time of the fade to the time of nearest maximum or minimum. Except for this additional step, the scaling procedure was as described above.

While duration and average visibility are the two most important quantities needed to describe a visibility fade, a third quantity, called fade importance, was found useful for many statistical applications; it was defined as follows:

$$\text{fade importance} = (1 - \text{average visibility}) \times \text{duration}.$$

The units of fade importance are those of time, but as a combination of visibility and duration in one quantity, it is a relative measure of the total coherent energy lost during a visibility fade. Fade importance thus provides a single quantity which can be used as an indication of the integrated deterioration of radio-star seeing conditions during visibility fades.

---

[1] This occurred especially when the ray-path from the star was most nearly parallel to the interferometer baseline. At such times, approximately thirty minutes are required for the star to traverse one fringe.

B. Distributions of Visibility-Fade Occurrence

Using the above definitions and the results of the above-described scaling procedures, certain statistical properties of visibility fades observed beneath the auroral ionosphere have been determined. In particular, studies have been made of the occurrence distribution of fades as a function of importance and as a function of time and space.

1. Importance distribution

In order to describe fully the occurrence distribution of radio-star visibility, it would be necessary to make a great number of visibility calculations, add up the total time that each value of visibility occurred, and present the data as a plot of visibility versus total time. Without automatic reduction techniques, such an approach would be totally impracticable for analysis of anything approaching a complete year's data. Essentially the same information can be obtained by sampling the records at times of known visibility reduction and then presenting the visibilities and durations observed. The form of presentation chosen for this report was that of plotting number of visibility fades versus fade importance for the year studied. While losing the autonomy of visibility and duration, this technique yields the convenience of a single variable as a measure of the severity of fades. This form of presentation may be of direct use in predicting the importance of ionospheric degradation of satellite tracking and communications reliability at VHF.

2. Time distributions

The time distribution of visibility fades at College has been studied by plotting the annual and diurnal variation of fade occurrence. An attempt was made to refine the technique and extend the results by making several such plots for various values of fade importance. It was found, however, that breaking the data into a sufficient number of importance groups resulted in groups too small to be statistically significant within themselves. Only the annual and diurnal distrubutions of total fade occurrence, therefore, have been retained.

3. Spatial distribution

Several techniques were attempted for analysing the spatial distribution of fade occurrence. Ultimately, it was found that a recognizable pattern emerged from the data only when the most direct approach tried was employed. The approach was simply to plot number of fades versus hour angle for each of the two radio stars observed - Cassiopeia A and Cygnus A. This technique combines both sky coordinates (in the form of hour angle and star-declination) into a single curve. It also averts systematic errors such as the fact that astronomical sources do not spend equal time in equal increments of azimuth (except, of course, for observations at the geographical poles). A complete year's data were used in order to separate positional from diurnal effects; such a separation ensues automatically in the course of a year due to the relationship of solar and sidereal times.

C. Frequency Dependence of Visibility Reduction

In order to study the frequency dependence of radio-star visibility, one month's records from the College 456 MC, 91.44-meter-baseline, interferometer were inspected during and near each fade recorded on the 223 MC instrument. If a simultaneous reduction in visibility lasting longer than a few scintillations was detected on the 456 MC record, the record was scaled in the manner described in Section III A. "Simultaneous" was taken to mean beginning earlier than one minute after the end of the 223 MC fade and ending later than one minute before the start of the 223 MC fade. The duration of each 456 MC reduction was determined and its fade importance calculated (whether or not the reduction qualified as a fade by the criteria of Section III A). Then, for each 223 MC fade, the relative importance observed on 456 MC to that observed on 223 MC was calculated by taking the ratio of the two fade importances. The distribution of relative importance was plotted and is presented in Section IV D.

D. Comparisons with other Geophysical Phenomena

To obtain some description of ionospheric conditions during visibility fades, certain geophysical records obtained at College and at other Alaskan stations were inspected. Magnetic K-indices at College were used as a measure of general geophysical activity, and 27 MC cosmic-noise absorption at College was used as a relative indicator of total ionospheric content.

Two specific phenomena - visual and radar aurora - were investigated for possible interdependence with visibility fades. Benson (1960) had reported a close time correspondence between extreme phase scintillation and the motion of each of two visual auroral forms through the field of view of the observing radio interferometer. In order to investigate the likelihood of a mechanismic relationship between radio-star visibility fades and visual aurora, a statistical analysis was made of auroral activity levels during recorded fades. The compilation of College all-sky camera records by Tryon (1959) was used for this purpose.

Due to the similarity of mechanisms know to produce radio-star scintillation and radar auroras - ionospheric forward scatter in the one case and backscatter in the other - a search was made for evidence of the common origin of radio-star visibility fades and radar auroras. In order to investigate the possible relationship, use was made of data collected by a chain of auroral radars operated in Alaska during the IGY (Leonard, 1961). The data inspected were in the form of punch-card tabulations of auroral backscatter return rate from radars operated at King Salmon, Farewell, and College. Return rates were available as the number of frames per hour of radar film (used at fifty frames per hour) which showed backscatter echoes in each of twelve, one-hundred-mile, range categories. The analysis technique used was to compare the return rate for a particular radar and range during particular

fades with the mean return rate for all observed times for that radar and range. For each radar and range, fades were chosen which might reasonably have been caused by scattering within the antenna beam of the radar and within the pertinent range limits.

Application of the technique described above, of course, required knowledge of which radars, if any, were illuminating the likely originating region of each fade and the range of the region from the radar; figure 5 displays the geometry involved in the necessary calculations. The geometry is that arising from a plane-earth assumption, which seems justified in the wake of such uncertainties as lack of precise radar antenna patterns and of known heights for the fade-origin regions; the calculations comprise a transformation of fade-origin position from interferometer to radar coordinates.

In figure 5, O represents the radar site, P the fade-origin location, and Q the interferometer. Fade-origin height is represented by H, and radio-star direction is given by azimuth, A, and zenith angle, Z, measured at the interferometer. Distance from the radar to the interferometer and azimuth of the interferometer measured at the radar are given by S and β, respectively. The fade-origin position is given in radar coordinates by zenith angle, Z, azimuth, θ', and range, R. θ' is measured from the direction of the radar antenna-pattern axis, which corresponds to geomagnetic north, while A, β, and θ are measured from geographic north. (The geomagnetic declination of all three radar sites was taken as

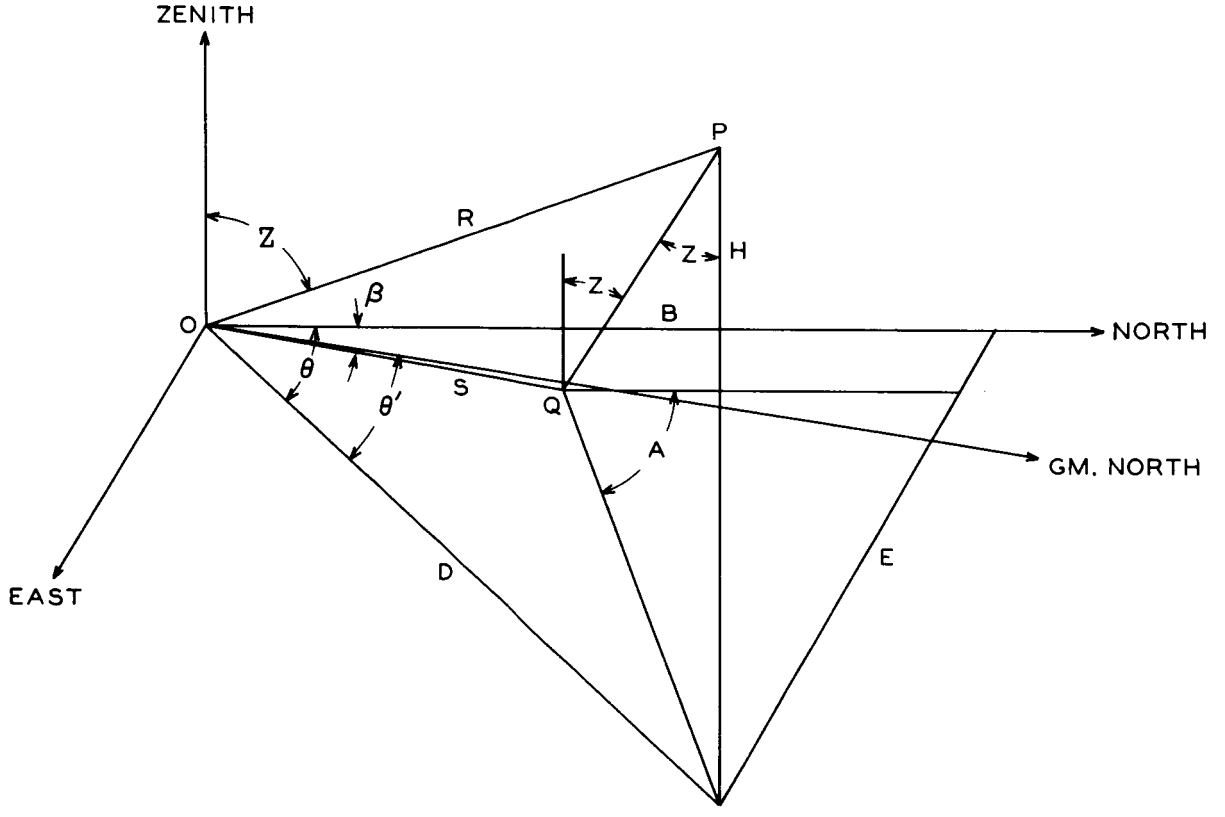

Fig. 5. Geometry for Conversion from Interferometer to Auroral-Radar Coordinates.

twenty-eight degrees east.) D, in figure 5, represents the ground projection of R; B is the north projection of D; and E is the east projection. The required coordinate transformation results from the following simple trigonometric calculations:

$$E = S \sin \beta + H \tan Z \sin A$$
$$B = S \cos \beta + H \tan Z \cos A$$
$$D = (E^2 + B^2)^{1/2}$$

$$R = (D^2 + H^2)^{1/2}$$
$$\theta = \sin^{-1} (E/D) \qquad \theta' = \theta - 28^\circ$$
$$Z = \tan^{-1} (D/H)$$

E. Computer Programs

For practical purposes, the above simple calculations were complicated by the large number of fades for which transformations were desired, an ideal situation for the University of Alaska's IBM 1620 digital computer. Accordingly, a program for the 1620 was written to carry out the above basic calculations. It was used in conjunction with another program written to perform certain other manipulations. Together, the two programs made it possible to compare visibility-fade and radar-aurora data systematically and provided program versatility for other purposes.

In particular, the combined programs provided calculation of radio-star hour angle from the date and occurrence-time of each fade, printout of the hour angle, and conversion of hour angle and declination into zenith angle and azimuth, as

required for the basic calculations listed above. In addition the program directed the computer to examine the results of each set of basic calculations to determine whether or not the point described was located within the main lobe of each radar antenna pattern and within the active range limits of each radar. Fade-origin position was then ignored or printed out in the coordinates of one, two, or all radars according to whether the result of each examination was negative or positive. The typed output of the computer included the following information:

Month	Fade number	Radio-star hour angle at time of fade
Radar number 1	Azimuth	Range
Radar number 2	Azimuth	Range
Radar number 3	Azimuth	Range

Radars were numbered as follows: 1 = King Salmon, 2 = Farewell, 3 = College. Any radar not illuminating the fade-origin position within its main lobe and between its range maximum and minimum was eliminated by the computer and absent from the printout. The hour-angle printout was included to provide data for the positional distribution of fade occurrence.

All the input data required for the above computer calculations were available as known constants or measured variables with the exception of fade-origin height. Height, of course, is one of the unknown parameters of interest, desired as a result of the present study. It is to be

remembered, however, that the purpose of comparing fade data with radar-aurora data was to demonstrate the existence or lack of evidence for the common origin of the two phenomena. With this purpose in mind, the established height of auroral backscatter - 110 kilometers (Leonard, 1961) - was used for the above calculations. The result of the comparison, of course, discloses the degree of validity of the height assumption.

The computer programs described above are presented in Fortran language in Appendix I. It will be noted that no calculation of zenith angle in radar coordinates is actually included in the programs. The necessity for such a calculation was precluded by the fact that, for a particular height, specification of range automatically includes specification of zenith angle. Hence, calculation and printout of azimuth and range was sufficient to establish completely the position of any 110-kilometer-high fade within the antenna pattern of a given radar.

The first of the programs presented in Appendix I was used also to calculate hour angle at times of record commencements, interruptions, and terminations for purposes of tabulating data availability to be used in correcting the observed positional distribution of fade occurrence. Output of this program was controlled by the sense-switch statement. This statement allowed operator choice of immediate printout of hour angle (for the data availability application) or card punchout of the information for use in subsequent calculations

and printout (for the observed position distribution and radar-aurora applications).

A simple program for compiling 27 MC riometer data was written for use in comparing fade occurrence with ionospheric absorption. It is presented in Appendix II.

IV. RESULTS

A. Importance Distribution

During the one year for which interferometer records were inspected, an average of about one visibility fade per day was found on 223 MC.[1] The most severe fade was one reported by Little, Merritt, Stiltner, and Cognard (1957), which reduced the visibility of Cyg A to an average of 0.3 for 84 minutes, yielding an importance of 59 minutes.[2] For the remaining 362 fades, the importance was essentially normally distributed, as shown in figure 6. Recalling the definition of fade importance, it is apparent that the most common fades - of importance around two minutes - typically represent approximately a half-reduction in radio-star visibility for a period of about four minutes. For purposes of data reduction, the importance of minimal fades (duration three minutes, visibility 0.5, importance 1.5) was rounded off to two, so that many of the fades included in the first data point of figure 6 were, in fact, minimal fades.

B. Time Distributions

The distribution of fade occurrence in time is presented in figures 7 and 10, the former showing the annual distribution as the average number of fades per data day for each

---

[1] No correction for missing or unuseable data.

[2] It is possible that a fade of 105-minute importance occurred. Evidence of equipment trouble, however, has left its validity questionable.

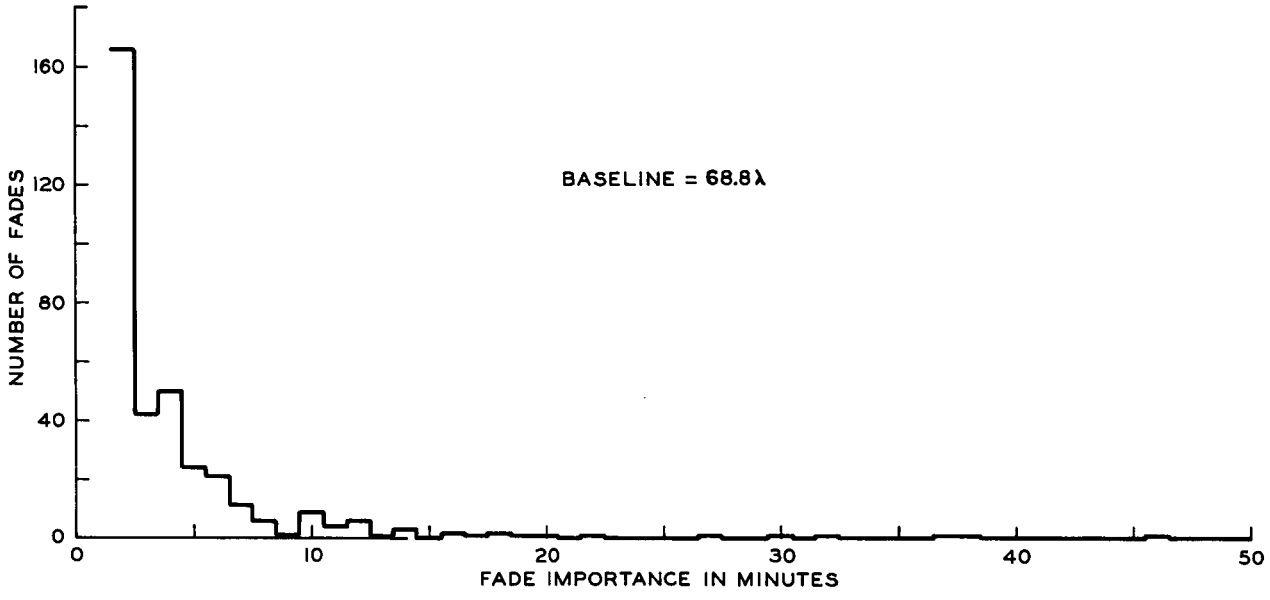

Fig. 6. Importance Distribution of 223 MC Visibility Fades Observed During One Year.

month and the latter giving the daily distribution as the average number of fades per full year of data for each hour. The terms "per data day" and "per full year of data" indicate that the plots have been corrected for lost observing time. That is, the ordinate corresponding to each date in the annual distribution is based on the same number of hours of observation (24), and the ordinate corresponding to each hour in the daily distribution is based on the same number of days of observation (365) during that hour. With one exception, the loss of observing time was sufficiently small and sufficiently well distributed in time of day and year that such correction clearly results in a valid distribution curve. The one exception was the month of February, 1958, during which difficulty with the interferometer's local oscillator resulted in considerable lost and unreliable data. Accordingly, February has been omitted from the annual distribution; the reliable data which are available from February show no striking departure from the distributions indicated by the other eleven months.

1. Annual distribution

The most noticeable feature in the annual distribution of fade occurrence is an autumnal maximum, which peaks, on figure 7, during the month of November, 1957. A fortunate fact resulting accidentally from the choice of observing period is that two such autumnal maxima are present in the data. That is, in spite of the fact that the observations from which data were used began on November 1, 1957, and

ended on October 31st, 1958, no serious discontinuity in the autumnal maximum ensues. The lack of a discontinuity, of course, indicates a repetition of the maximum, thereby lending verification of its existence as an annual feature.

Due to the considerable variation in number of fades occurring on consecutive days, it was necessary to average over at least several days in order to obtain a reasonably smooth annual distribution; figure 7 is the result of such averaging for periods of one month. The result of a shorter averaging period is shown in figure 8. It is evident that an averaging period of less than one week is not quite sufficient to overcome random variations in one year's data. To the extent that such an averaging period produces reliable results, however, the autumnal maximum appears to peak early in November. The lack of discontinuity between the last period in October, 1958, and the first in November, 1957, again lends some weight to the likely reality of such a peak in the face of the deep depression in the curve (assumed randomly produced) during the second and third averaging periods of November, 1957. If the early November peak in the autumnal maximum is genuine, it is seen to occur quite nearly midway between the autumnal equinox and the winter solstice.

With a yearly component in fade occurrence established, one is disposed to looking for a semi-annual component. The possibility of such a component is suggested in figure 7 by the month of May, 1958. The increased rate of occurrence during May, however, is not large enough to preclude a

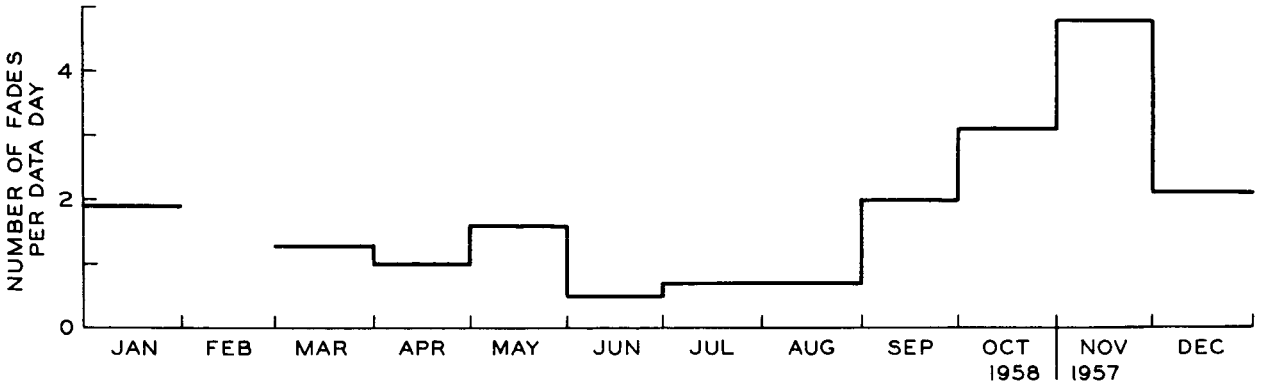

Fig. 7. Annual Distribution of 223 MC Fade Occurrence (monthly averages).

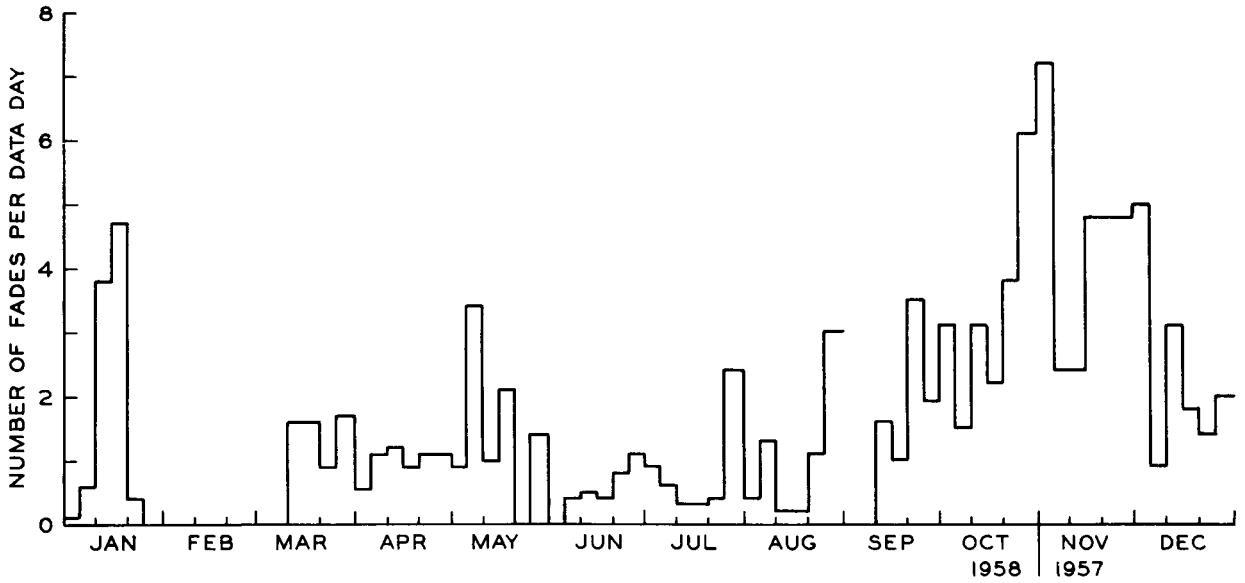

Fig. 8. Annual Distribution of 223 MC Fade Occurrence (quasi-weekly averages).

reasonable doubt about its validity as an annual feature. Further, only one year's data are present in the spring period of figure 7 in contrast with the inclusion of two different year's data in the autumnal maximum. Nevertheless, an interesting point is raised in figure 8 concerning the possible existence of a spring maximum. The feature in question is the rather sharp peaking of the alleged spring maximum during the second five-day period of May; the peaking occurs quite precisely midway between the spring equinox and the summer solstice. It is pointed out that the peak was caused almost entirely by a large number of fades which occurred on a single day, during which the condition of the ionosphere may well not have represented the usual condition for that time of year. A spring maximum in fade occurrence, therefore, must be considered only as suggested by the data in contrast with the autumnal maximum, which may be considered quite well established.

Concerning any apparent annual variation in occurrence of visibility fades, however well established, the question immediately arises as to whether the variation represents a true annual change in ionospheric conditions or rather occurs due to some annually varying condition of observation. In particular, it would be reasonable to expect an effect due to a coincidence, during some part of the year, of positional and diurnal maxima in fade occurrence. That is, during the time of the year when the radio star was in a favored fade position at a favored time of day, one might expect to observe

an increase in the number of fades occurring per day even in the absence of any real annual variation in ionospheric conditions. It is a simple matter to test for such an effect by using two radio stars which are displaced from one another by a sufficient amount in right ascension. Cassiopeia A and Cygnus A satisfy this requirement, being displaced by about three and one-half hours in right ascension. Figure 9 shows the annual distribution of fades for each of the two stars independently. The program of observation from November, 1957, through June, 1958, consisted of switching from one radio star to the other at intervals of four days, while observations from July through October, 1958, used the Cygnus source exclusively. Fortunately, the lack of Cas data during the latter period of observations is not important for present purposes.

Due to the three and one-half hour difference in right ascension between Cygnus and Cassiopeia, any annual variation in fade occurrence arising from superposition of diurnal and positional effects would display about a two month lag of the Cassiopeia curve relative to the Cygnus curve. No such lag exists in the autumnal maxima of the two distributions shown in figure 9; the Cygnus distribution peaks in November, and the Cas distribution peaks no later than November. In the spring, there is a one month lag of the Cas maximum compared with the Cyg maximum when the distributions are presented, as in figure 9, on the basis of a one-month averaging period. It is possible that a shorter averaging period would produce

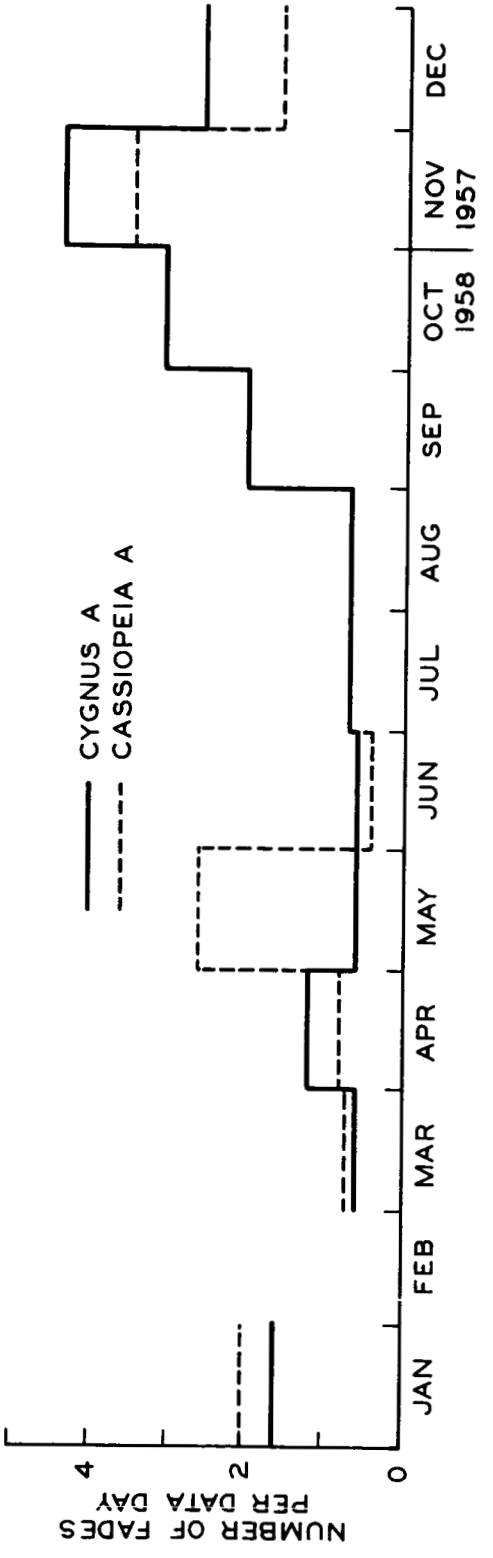

Fig. 9. Annual Distribution of 223 MC Fade Occurrence for Cygnus and Cassiopeia Independently.

more nearly the required two-month lag. As pointed out in discussion of figure 8, however, shorter averaging periods result in marginally reliable distributions even when data from both stars are used; the condition is worsened for single-star distributions because of the inherently smaller statistical sample involved in each curve and because of the four-day period of alternation between stars. Once again, then, the spring maximum in occurrence level must be left in an uncertain state compared with the autumnal maximum. It is noticeable that the existence of a spring maximum is much more evident in the independent Cassiopeia distribution than in the combined distribution of the two stars. Again, however, this is due largely to contribution from a single day.

2. Diurnal distribution

In order to study the diurnal distribution of fade occurrence, it is necessary to combine data from one full year (or an integral number of years) so that any positional distribution will be smoothed out. In the case of the data used in the present study, it was necessary also to use only records obtained from the Cygnus source due to the absence of Cassiopeia data during the last four months of the observations. Simply restricting the data used in the diurnal study to that obtained with the Cygnus source, however, would be self-defeating as an attempt to purge the result of positional bias. Such a procedure would give disproportionate weight to the part of the year during which Cygnus was observed continuously as compared with that part during which it was

observed intermittently at four-day intervals. This effect can be counteracted by weighting the data from the intermittent part of the year twice as heavily as that from the continuous part of the year; the intermittent nature of the former data is itself unimportant, the relative change in sidereal and solar time during any four-day period being insignificant in this regard.

The diurnal distribution resulting from analysis of the Cygnus data is presented in figure 10. The most prominent feature of the distribution is the obvious early-morning maximum, which reaches a peak about two hours after local midnight. Figure 10 is inherently an average diurnal distribution of fade occurrence since a whole year's data were used in its construction. The question of change, during the course of the year, in the diurnal distribution of fades naturally arises. The year's observations did not give a statistically significant number of data in any month and only marginally so in any season to describe such a change directly. It is possible, however, to infer the extent of such a change by manipulation of the ordinates of figure 10. The manipulation consists of multiplying the contribution of each month to the ordinate by a factor which is inversely proportional to that month's level on the annual occurrence distribution. Such a procedure results in an average diurnal distribution - figure 11 - in which the contribution from each

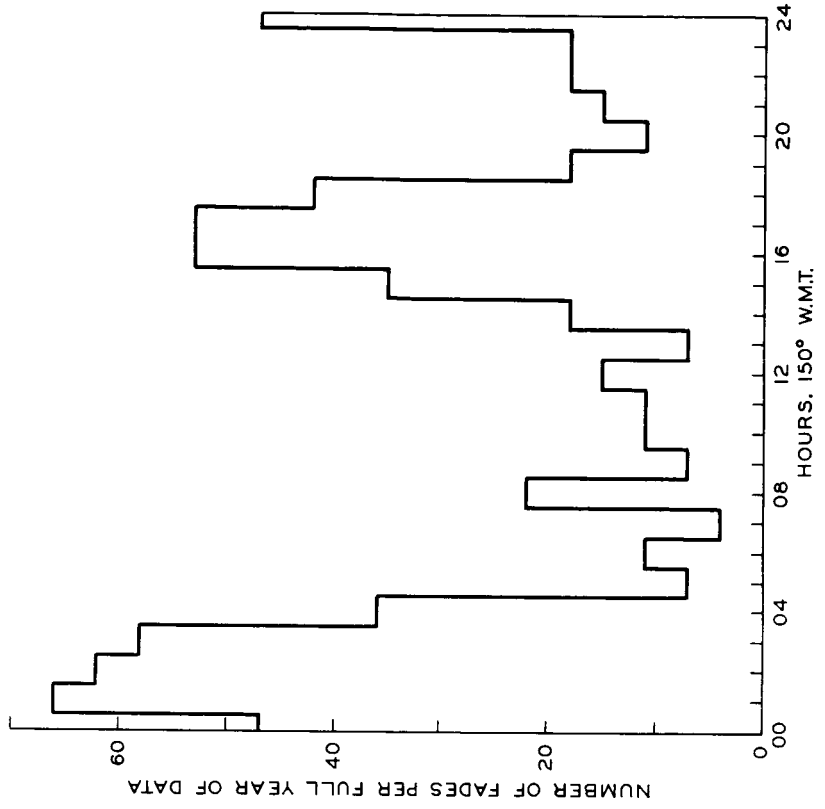

Fig. 11. Diurnal Distribution of 223 MC, Cygnus, Fade Occurrence Weighted to Suppress Annual Variations.

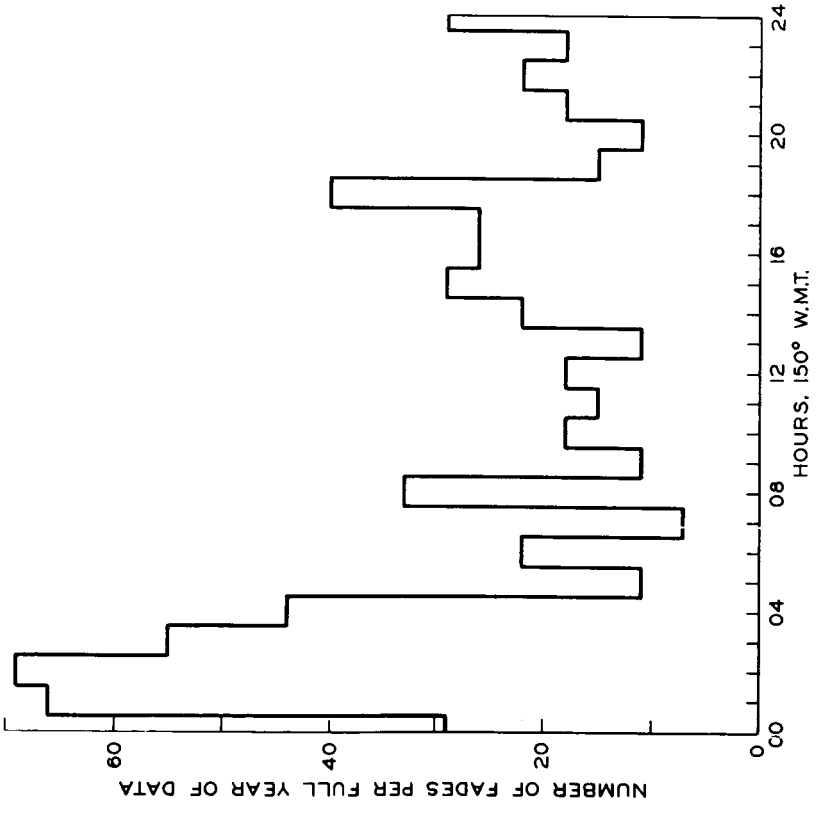

Fig. 10. Diurnal Distribution of 223 MC, Cygnus, Fade Occurrence.

month is equal. In contrast, the respective contributions to figure 10 are weighted according to the relative monthly occurrence levels.

Arguments can be invoked for presenting the diurnal distribution in either of the two manners described above; they are both yearly averages and one or the other may be preferable for certain purposes. For the present discussion, it is the difference between the natures of the two presentations rather than the nature of either which is important. The difference in nature will produce a noticeable difference in shape of the two distributions if any significant annual change in diurnal pattern exists. Comparison of figures 10 and 11 reveals immediately that there is some seasonal variation in diurnal distribution of fade occurrence. The ordinate manipulation carried out to produce figure 11 strongly emphasizes the afternoon maximum suggested in the distribution of figure 10. If one thinks of figure 11 as representing the "normal" diurnal distribution of fade occurrence, then the difference between it and figure 10 implies that the "abnormal" seasonal periods of enhanced occurrence bring with them a flatter diurnal distribution. That is, fades tend to occur at two peak times of day during most of the year but more at any time of day during the active months. It is to be noted that, while the afternoon peak smooths out during active months, the early-morning maximum appears to persist throughout the year.

C. Spatial Distribution

The techniques by which the positional distribution of fade occurrence were studied are similar to those employed for the diurnal studies. The reason for similarity in techniques is obvious if one uses source hour-angle as the basis for positional study, since the positional distribution then is tantamount to a distribution of fade occurrence in sidereal time. It is sufficient to say, then, that a positional distribution must be constructed from data collected over one or more full years from a source which is observed consistently[1] and that it must be corrected for any variations in availability of those data. Accordingly, the resulting distribution is an average one and may be presented with or without a correction for seasonal variation of activity as described in the discussion of figures 10 and 11. Two such average distributions, using Cygnus data from 1957-58, are presented in figures 12 and 13, the latter including the seasonal correction. In contrast to the case for diurnal distribution, there appears to be little difference between the two positional plots, indicating little or no seasonal change in positional distribution.

Two prominent features are evident in both figures 12 and 13, a sharp maximum at zero hour-angle and a broader, less pronounced one to the west. Interferometer geometry by itself

---

[1] Interruptions must be kept short compared with the period required to produce a significant "slip" between solar and sidereal time.

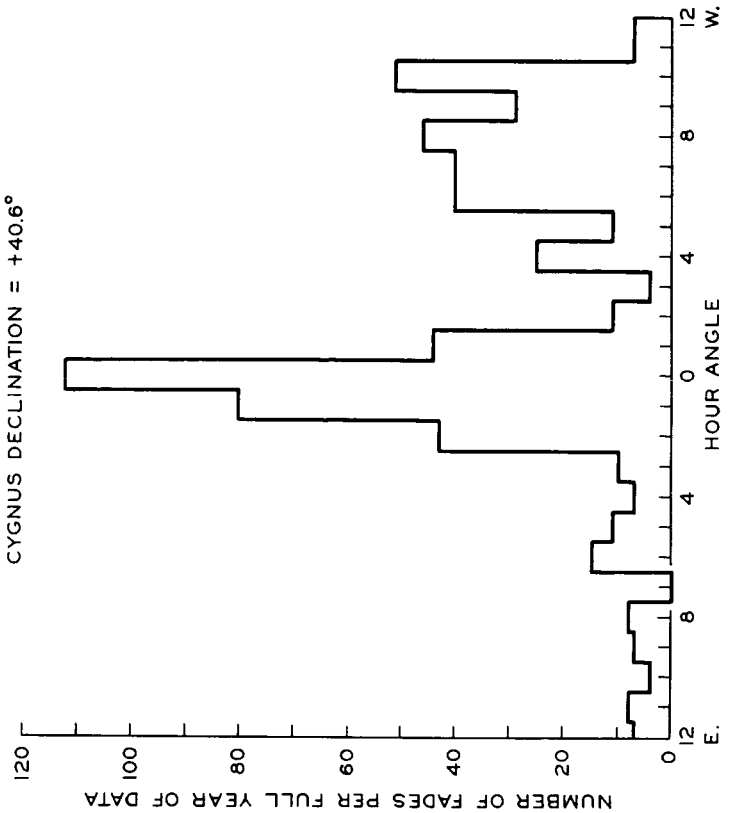

Fig. 13. Directional Distribution of 223 MC, Cygnus, Fade Occurrence Weighted to Suppress Annual Variations.

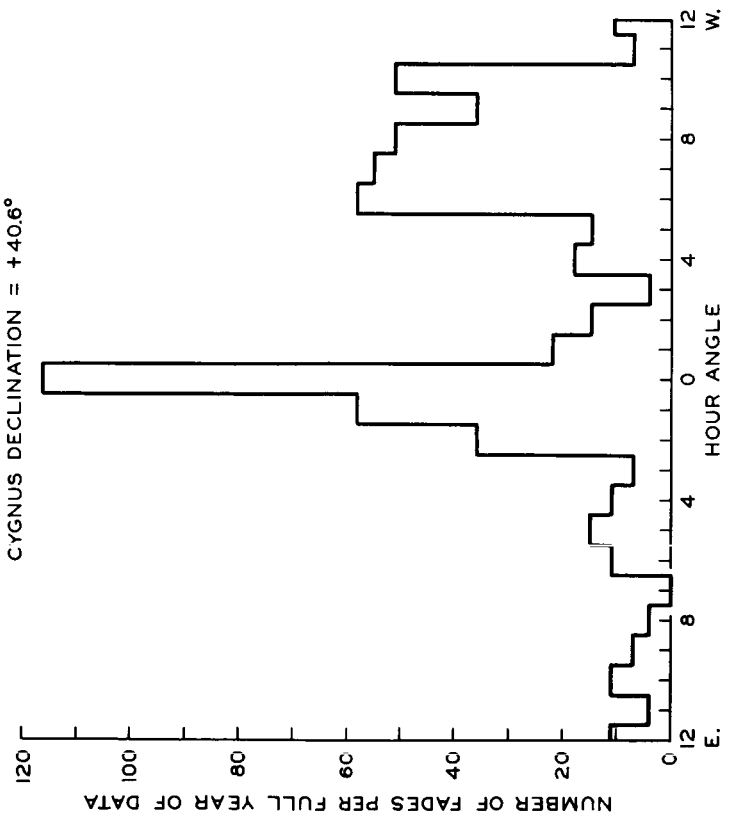

Fig. 12. Directional Distribution of 223 MC, Cygnus, Fade Occurrence.

could produce two maxima in the positional distribution of visibility fades for circumpolar radio stars. As the source moves through the sky, the projection of the interferometer baseline on the normal to the arriving ray path continuously changes. This projection, which represents the effective antenna spacing for the interferometer reaches two equal maxima during a sidereal day, one each time the ray path is perpendicular to the baseline. Maximum effective spacing produces optimum instrumental conditions for loss of correlation between signals arriving at the two antennas and hence for the occurrence of visibility fades. For the case of the College interferometers, which have east-west baselines, maximum effective spacing occurs at upper and lower transit of circumpolar stars. An approximately equal pair of occurrence maxima at hour angles of zero and twelve, then, could be explained purely on the basis of observational geometry.

Figures 12 and 13 obviously display one of the geometrically-expected maxima, but there is not the slightest suggestion of the other. The absence of an occurrence maximum at lower transit clearly implies that the maximum experienced at upper transit is of geophysical significance. The broad maximum experienced at west hour angles is not to be expected on the basis of instrumental geometry and must be viewed as arising solely from ionospheric effects. An interpretation of figures 12 and 13 is discussed in Section V.

D. Frequency Dependence of Visibility Reduction

The results of a one-month comparison of visibility data on two frequencies are presented in figure 14. For the month of December, 1957, records from the 456 MC phase-switch interferometer were inspected for decreases in visibility at the times of known 223 MC visibility fades. When any decrease was detected (whether or not it would have been sufficient to qualify as a fade by the criteria established), its importance was calculated according to the definitions of fade importance. Figure 14 displays the number distribution of 223 MC fades as a function of the relative importance of 456 MC visibility decrease to 223 MC decrease. That is, the abscissa of figure 14 is the ratio of 456 MC importance to 223 MC importance at the time of 223 MC fades. The distribution is seen to be quasi-normal, peaking at a relative importance of 0.2.

It must be pointed out that figure 14 does not present the entire observed relationship between visibility reduction on 223 MC and 456 MC; systematic inspection of all records from the 456 MC interferometer for the month of December, 1957, revealed several instances of visibility decrease on 456 MC with no corresponding decrease on 223 MC. The month of December, 1957, was not specifically picked for frequency comparison; it simply was the first month for which records were examined and may be considered as randomly chosen.

E. Comparison with other Geophysical Phenomena

1. Magnetic K-index

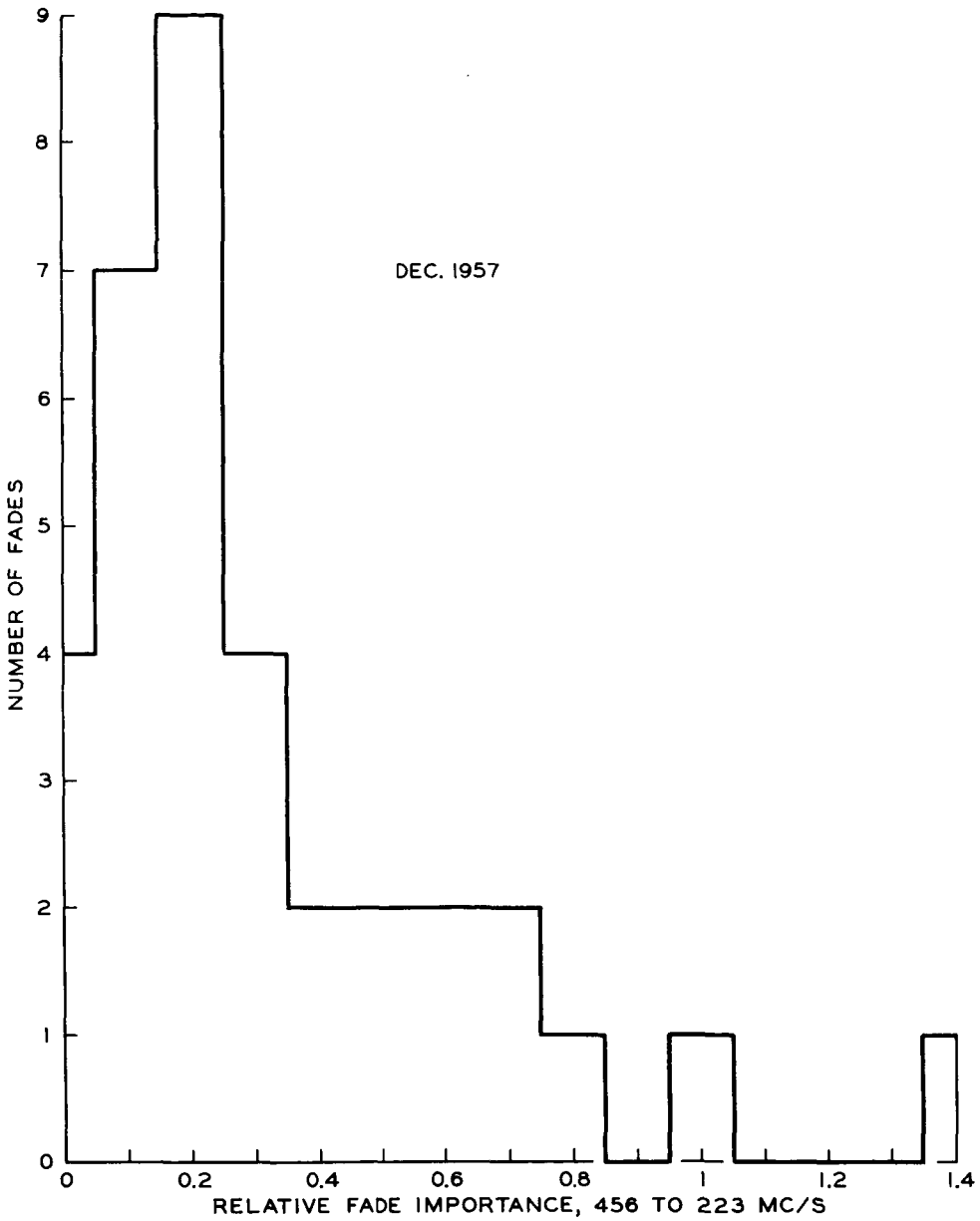

Fig. 14. Relative Importance of 456 MC to 223 MC Visibility Reduction.

In addition to the distributions of visibility fades in time and direction from the observing point, occurrence was studied as a function of several measureable geophysical quantities. The first of these to be presented is magnetic K-index. For the time of each visibility fade observed on 223 MC, the 3-hour K-index for College was recorded; the number of fades which occurred during periods having each integral value of K was then determined. The resulting fade distribution as a function if K-index is presented as the solid curve of figure 15. Such a distribution is of no value, of course, unless the relative rates of occurrence of the K indices themselves is known; this information is presented by the dashed curve of figure 15. The dashed curve gives the fade distribution which would be expected if no K-index dependence of fade occurrence existed. Comparison of the two curves shows that the observed distribution is quite similar to that expected for no dependence except for a statistically marginal excess of observed fades at very high magnetic activity levels and a somewhat sharper peaking of the observed curve at K-index = 2. The sharper peaking is of sufficient degree to imply a possible preference for moderate magnetic activity levels.

Because of the inconclusive nature of figure 15, a second investigation of K-index dependence was made, using fade importance rather than occurrence rate as the dependent variable. The importance factors for the fades occurring during each value of K-index were added together and the sum

divided by the number of fades in each group to give the average importance of all fades occurring during each level. The results of this procedure have been plotted in figure 16. No magnetic dependence would result in a flat distribution of importance as a function of K-index. Hence, figure 16 shows that when average importance is used as the criterion, there is a definite preference for moderate magnetic activity levels. The importance criterion, then, corroborates the tentative conclusion of the occurrence criterion although the actual peaks of the two distributions differ by one integral value of K-index.

2. Cosmic-noise absorption

Comparison of fade occurrence and relative electron density of the ionosphere was carried out by plotting number of fades against absorption level measured at 27 MC by the College vertical RIOMETER (relative ionospheric opacity meter), which is a sensitive indicator of electron density in the lower E layer and upper D region. The method of comparison was similar to that described above for comparison with magnetic K-index except for the number of data involved. Data were available in convenient form (tabulations of 15-minute samples of absorption) for only part of the year. On the other hand, the quarter-hour intervals between riometer data samples as compared with the three-hour interval of averaging for K-index resulted in many more data points being available for construction of a "no-dependence" curve

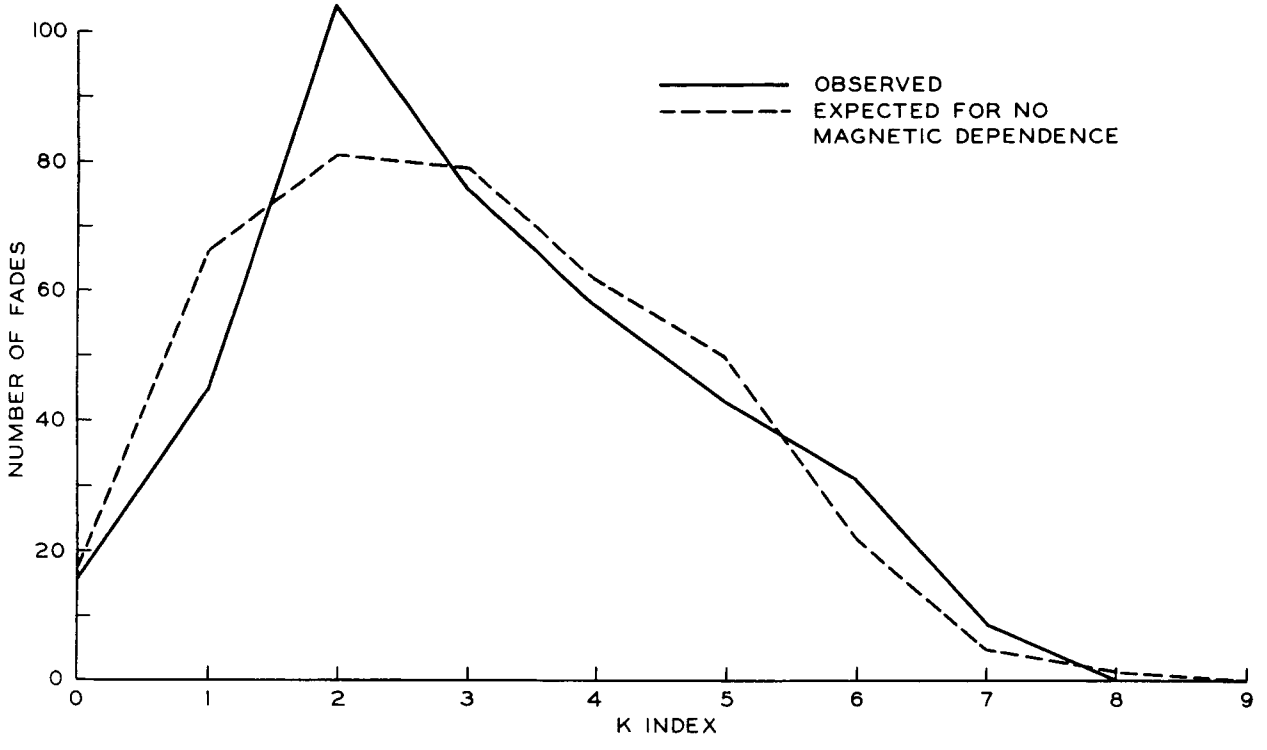

Fig. 15. K-Index Distribution of 223 MC Fade Occurrence.

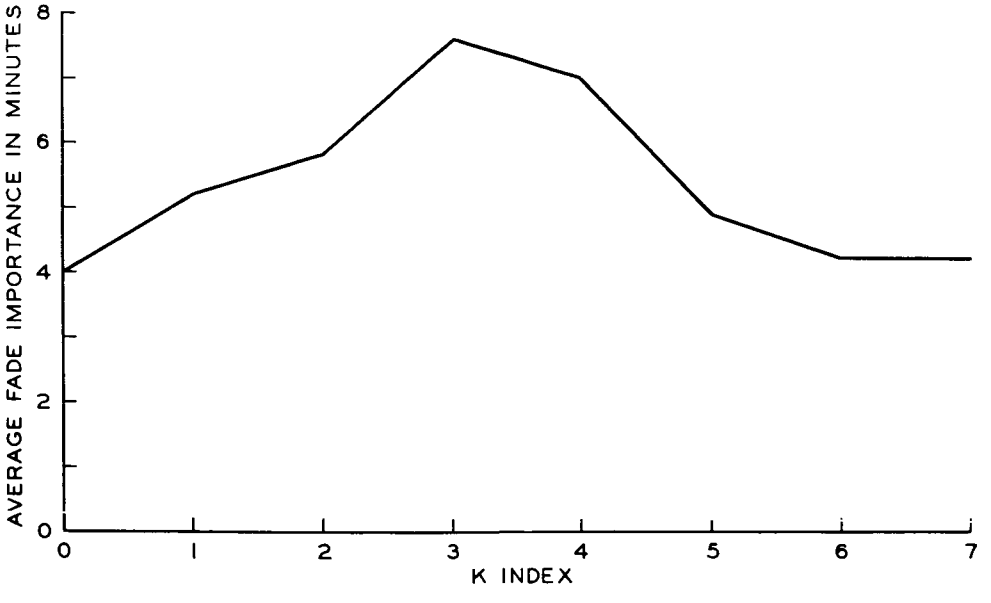

Fig. 16. K-Index Distribution of 223 MC Fade Importance.

than was the case in figure 15. A simple program[1] was devised, therefore, for the University of Alaska IBM 1620 digital computer to provide automatic compling of riometer data from which to construct the no-dependence curve of figure 17.

The observed distribution of fades with absorption level is represented by the solid curve of figure 17. It was established in the same way as that of figure 15 except that ordinates are averages of five data points, whose absissas are separated by one-tenth of one decibel, whereas the ordinates of figure 15 are discrete data points. This minor difference in presentation arises from the different natures of the K-index and absorption data used. The averaging in figure 17 was necessitated by the smaller total number of fades involved due to several missing months of convenient absorption values.

In spite of the slightly different methods of presentation used in figures 15 and 16 on the one hand and figure 17 on the other, a similarity of results is to be noted. In both cases, the most evident departure of the observed curve from the no-dependence characteristic is a slight preference for moderately disturbed conditions (K index of 2 to 4 and absorption of 1 to 2 db) at the expense of completely quiet conditions. In both cases, also, there is no clearly evident enhancement of fade occurrence for highly disturbed conditions.

---

[1] The Fortran program is given in Appendix II.

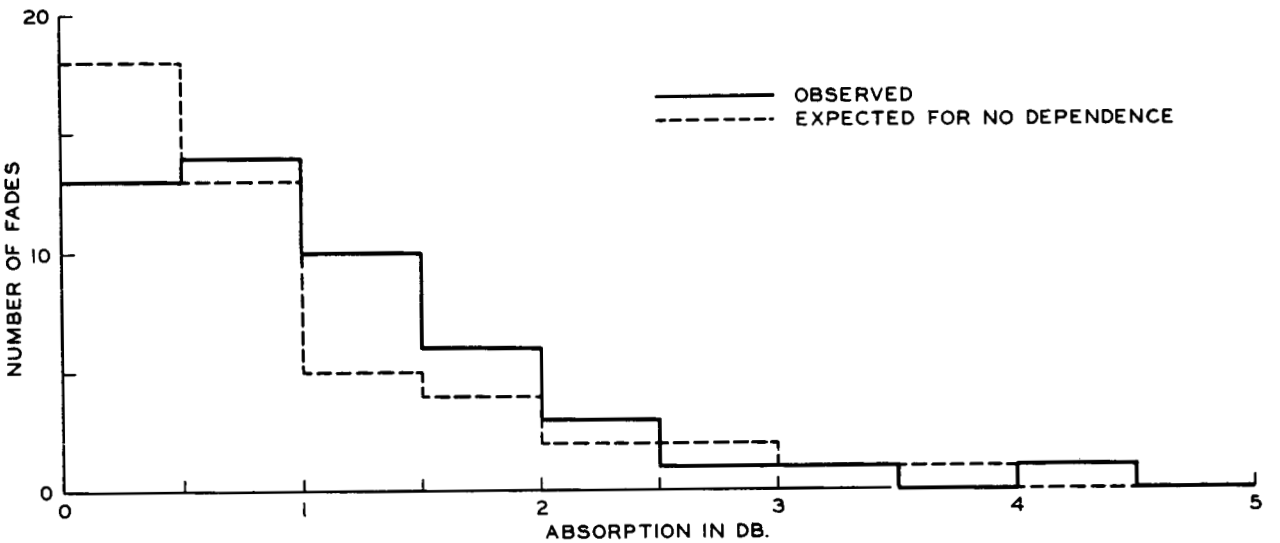

Fig. 17. Distribution of 223 MC Fade Occurrence with 27 MC Cosmic-Noise Absorption Level.

3. Visual aurora

Statistical investigation of interdependence between visibility fades and visual auroras was rendered questionable by limited availability of the most useful type of auroral data - tabulations of auroral indices from all-sky camera films. A one-year study is hardly sufficient to establish the existence or lack of a dependence because of the many hours of daylight, moonlight, and cloud cover. Such factors reduce the availability of auroral data well below that from more continuous measurements such as K-index and radio absorption. Nevertheless, various attempts at such a study were made. Such techniques as trying correlation of fade importance with auroral index failed completely to produce reliable results; due to data limitations, it was found that no subdivision of data into index or importance groupings was feasible.

Only a straight-forward comparison of fade occurrence and auroral occurrence produced even marginally significant statistics. Such a comparison revealed that of the 107 fades which occurred during times for which there are reliable all-sky camera data, forty were accompanied by aurora in the sky at least within fifteen minutes of the fade. The occurrence rate of aurora during (or nearly during) visibility fades, then, was thirty-seven percent. By comparison, the overall observed occurrence rate of aurora during roughly the period of time covered by this report was twenty-nine percent. The apparent enhancement during fades is comparable

with the probable errors involved in comparison and, in any case, is not striking.

4. Radar aurora

Compared with visual aurora, a relatively large enhancement of radar-aurora occurrence during visibility fades was found. The sharp peak near upper culmination in the positional distribution of fade occurrence had the effect of making the King Salmon radar the most important for the study described in Section IV D. Unfortunately, it was just this radar which experienced the most operational difficulty of the three of interest; it operated "at very reduced transmitter power" (Leonard, 1961) throughout most of the period covered by this report. The Farewell radar, however, did illuminate a number of possible fade-origin regions at times of interest and punched-card radar information was available for some of these cases.

Printout of the available Farewell cards resulted in eleven samples of reliable data for hours during which observed fades - if produced at 110 kilometer height - would have been produced within the main lobe of the antenna and between the active range limits of the radar. Of these eleven data samples, three showed no radar echoes at all; examination of the computed origin positions of these fades revealed that, while they were within the nominal main lobe of the antenna, all three were well outside the half-power beamwidth of the lobe.

The remaining eight data samples showed a mean radar return rate of 58% while the all-time mean return rate for the four range categories involved was 19%. Thus there was an enhancement of about threefold in radar return rate for the fade-associated data simples. Further, in each of the eight samples, the individual rate for the range category involved exceeds the all-time mean rate for that category. It is to be noted that including the three no-return data samples does not destroy the enhancement of return rate; it merely decreases it to about twofold. A special case of some possible significance is the one in which the calculated fade-origin position was closest to the center of the radar beam (one degree off-center in azimuth and at about the 90%-power point in elevation), which showed auroral backscatter returns from the calculated range category on 49 out of the 50 frames of data collected during the hour including the fade. High return rates were experienced from this and adjacent range categories for several hours preceding and following the fade.

In view of the above results from the few available tabulated radar data, a visual inspection of a small amount of film collected by the King Salmon radar was carried out. Such visual inspection does not lend itself to quantitative statistical study without the establishment of a relatively long-term, semi-automatic program of data reduction. Of the 49 fades for which film was inspected, however, 53% appeared to be associated with radar returns. The association was inferred from an identifiable trace which seemed to recur at

or near the times of these fades (within a few minutes in most cases). Characteristically, this trace was very faint and occurred somewhat closer to the radar (usually on the order of 100 kilometers closer) than the calculated range.

V. DISCUSSION

The stated purpose of this study was to investigate empirically the termporal and spatial statistics of radio-star visibility fades in the auroral zone and to establish the degree of relationship of fades with certain other geophysical phenomena. The data collected and reduced for that purpose have been presented and discussed in Section IV. Anything approaching a full theoretical treatment of the questions arising from the existence of such fades is beyond the scope of this paper; in this section, however, it is intended to point out some inferences which may be drawn from the empirical results. It is hoped that the discussion will provide a descriptive basis upon which later theoretical studies may be built.

Quite evidently, the most important result of the study herein reported was the discovery of the large number of visibility fades which had been recorded on 223 MC by the College interferometer between November, 1957, and October, 1958. It is to be remembered, of course, that the number of fades recorded by any instrument under any conditions depends upon the quantitative criteria used in defining a visibility fade and that there is no obvious natural line of demarkation between visibility fades as defined herein and lesser or less lengthy decreases in visibility of a radio star. Nevertheless, with the concept of fade importance available as a measure of

degradation in radio seeing conditions (as in figure 6), the visibility fade is seen to be a significant anomalous feature of the auroral ionosphere, at least during a maximum sunspot period.

The annual distribution of fade occurrence, shown in figure 7, may be construed to describe visibility-fade conditions more as "transitional" than as "anomalous." By this is meant that while fades do occur as unusual or anomalous events during any part of the year, they appear to represent a relatively common condition of the auroral ionosphere during the transition from summer to winter structure and possibly again during the opposite transition in spring.

The transitional state of the ionosphere during visibility fades is suggested not only by their annual distribution but also by their diurnal distribution, which is shown averaged over a year in figure 10. The prominent early-morning occurrence maximum corresponds precisely (within the limits set by averaging) with local magnetic midnight. A considerable collection of auroral data by Davis (1961) shows a type of transition - namely, reversal from predominantly westward to predominantly eastward motion - consistently taking place near magnetic midnight.

It is undoubtedly necessary to clarify what is meant by "transitional" in the above paragraphs. Certainly, no clear-cut idea of a particular ionospheric mechanism is meant; the term is to be taken in a general way. The only particular

feature of the "transition" (or the several kinds of transition) which seems evident in the data is that it is a more-or-less normal change from one condition of the auroral ionosphere to another, rather than a violent disturbance. Support for such a view seems to be contained in the distributions of fade occurrence with K-index and cosmic-noise absorption, both of which show preferences for mildly disturbed conditions and no significant enhancement during highly disturbed periods.

An additional suggestion of the transitional nature of visibility fades is made by comparison of the diurnal maximum of fade occurrence with that of visual auroral occurrence. Data collected at several Alaskan stations including College, during the auroral observing season of 1957-8 (Davis, 1961) display a maximum in auroral occurrence at or shortly before midnight, local time. The diurnal maximum in fade occurrence, then, follows that for visual auroras by about two hours. During the intervening time, the auroral occurrence level has fallen to about 70% of its peak value and the ionosphere presumably is in transition between disturbed auroral conditions and post-auroral conditions. In the jargon of auroral physics, radio-star visibility fades would appear to constitute a post-breakup phenomenon if related at all.

While the question of the existence of a relationship between visual aurora and visibility fades must be left open, there is little doubt concerning one with radar aurora. Although the number of simultaneous data available for

systematic comparison was quite limited, the numerical results were of sufficient magnitude to suggest a relationship between the two phenomena. Further, inspection of auroral radar film produced a qualitative result which is consistent with the known characteristics of ionospheric scattering. The relationship implied is that, at and near the time of fades, ionospheric irregularities exist which are of such scale and density as to promote severe forward scatter at VHF while acting as inefficient backscatterers at HF. Such a view ensues from the fact that fades seemed related to very weak radar returns and not at all to strong ones. Film frames exposed near fade times variously displayed moderate or strong returns before, during, or after the fade, closer to or farther from the radar than predicted, or not at all; on the other hand, a predominance of weak returns at or slightly closer than the predicted range was observed. The characteristic returns ranged in intensity upwards from the threshold of radar sensitivity, suggesting that absence of such returns possibly was due, at times, to observational limitations rather than to absence of the characteristic ionospheric conditions. Still, many factors - not the least of which is orientation of scattering irregularities - probably contributed to the lack of a one-to-one correspondence.

The recurring discrepancy observed between calculated and observed range in the cases of simultaneous or near

simultaneous fades and radar returns is of possible significance. Since the calculations, which were based on an assumed height of 110 kilometers, resulted in greater ranges than those observed by the radar, there is an indication of irregularities existing below the assumed height. A possible implication of this result is that radio-star visibility fades are related to radar auroras with unusually low lower borders, corresponding either to a lowering or to a thickening of the auroral-backscatter layer. On the other hand, the error introduced into the calculations by assumption of a flat earth is in the proper sense to explain the observed discrepancy. A quantitative check on this error has not been carried out.

While at least occasional contribution of E-layer irregularities to the production of fades is indicated by auroral radar data, the positional distribution of fades shows that higher irregularities are almost always involved. The presence in figure 12 of one geometrically induced occurrence maximum and the absence of the other clearly reveals either a latitude or an aspect-angle (or both) dependence of fade occurrence. Lower-latitude observations (Flood, 1962) have shown an increase in fade occurrence when the star signal is passing through the auroral ionosphere. Accordingly, an attempt has been made to explain the two maxima shown in figure 12 on the basis of auroral-ionosphere geometry. Inasmuch as there is no conclusive evidence that

the radar auroral zone differs appreciably from the visual zone, a model has been devised for interpretation of figure 12 on the basis of a scattering zone centered approximately on the visual auroral maximum. The maximum used was 66.5 degrees geomagnetic latitude, corresponding to that found by Davis (1961) during the 1957-8 auroral season in Alaska.

Figure 18 shows the position of Davis' maximum along with the approximate positions of his half-occurrence levels. A short line also has been drawn parallel to the auroral maximum and through the interferometer site at College. This line indicates the two azimuths for which the horizontal component of the Cygnus ray-path angle-of-incidence to the auroral zone is zero. Consider a system of irregularities confined to and uniformly distributed within the idealized auroral zone of the figure. If there were no change in vertical component of the ray-path incidence-angle with azimuth, maxima in fade occurrence would be expected in the directions indicated by the line. The vertical component does change, however, and the manner of its change can be implied from the track of the Cygnus ray-path on any level above the surface. The ground projection of such a track is shown for 100-km height in figure 18. The distance from College to the track projection is proportional to the tangent of the vertical component of the incidence angle. Comparing the distances for the two azimuths of zero horizontal component, it is clear that any fade-occurrence maximum tc

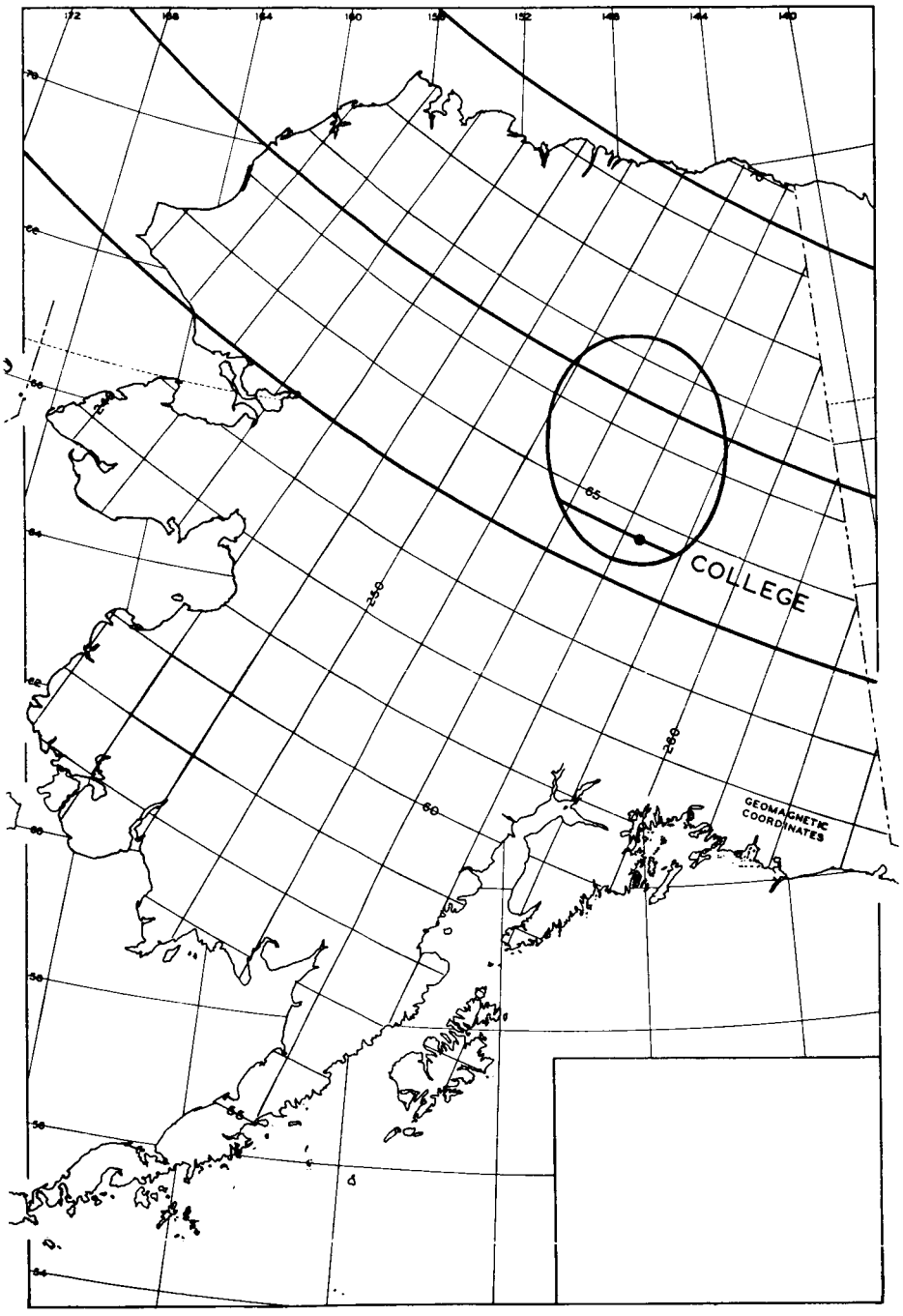

Fig. 18. Auroral-Zone Geometry with 100-kilometer Track.

to be observed in the westerly direction will be considerably stronger than any in the easterly direction. In fact, with the vertical component considered, a maximum in the easterly direction is not to be expected while one in the westerly direction is likely.

The two directions in question represent azimuths of approximately 120 degrees and 300 degress, corresponding to Cygnus hour angles of approximately 3 hours east and 7 hours west. The latter falls within the observed fade-occurrence maximum appearing at westerly hour angles in figure 12. The rudimentary model described above, then, appears to explain one of the observed maxima on the basis of auroral-zone geometry. The sharper maximum observed at upper transit will now be considered.

As discussed in Section IV C, the upper-transit maximum could be explained purely on the basis of instrumental effects if there were a corresponding peak at lower transit. In lieu of any other explanation for the upper-transit peak, it is necessary to investigate the absence of one at lower transit. First, it is obvious that if no scattering irregularities exist between the star and the interferometer, no fades will occur, regardless of effective spacing (provided it is not great enough to resolve the star). Accordingly, if the irregularities are confined to a definite zone, and if the lower-transit ray path does not pass through that zone, then no instrumentally induced maximum in fade occurrence is to be expected at lower transit.

Figure 18 shows that the lower-transit ray path does, in fact, pass through the idealized auroral zone described above if the zone is placed at a height of 100 kilometers. This fact is also shown in figure 19, which displays the pertinent geometry in a vertical plane through the College meridian. In figure 19, however, the scattering zone (lined region) is extended upward indefinitely from 100 km, approximately in the direction of the earth's magnetic field. The Cygnus ray paths at upper and lower transit are shown passing through the extended zone. The upper-transit path enters the zone at about 330 kilometers height, while the lower-transit path enters at about 180 kilometers. Irregularities confined to the zone and lying between 180 and 330 kilometers in height, then, will contribute to diffraction of the Cygnus signal at upper transit but not at lower transit. To the extent that the model represents the true latitudinal distribution of the scattering zone, therefore, it is suggested that irregularities between 180 and 330 kilometers are responsible for the large ratio of upper-transit to lower-transit visibility fades displayed in figure 12.

The above considerations do not include the important question of aspect angle between the ray path and any possible elongated axis of the scattering irregularities. It is pointed out that the geomagnetic zenith angle of Cygnus is less than 20 degrees at upper transit and near 80 degrees at lower transit, so that a strong aspect-angle effect could

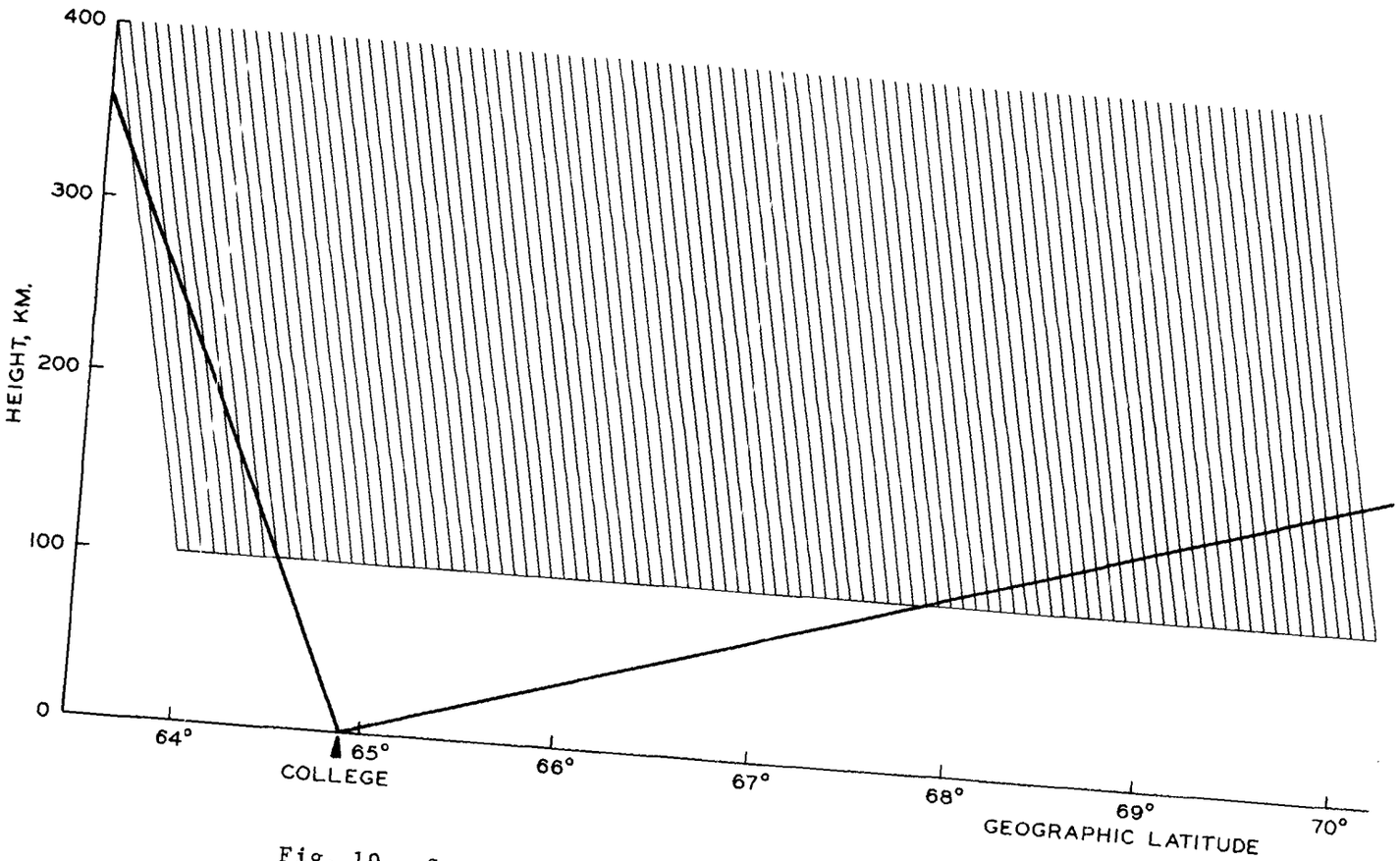

Fig. 19. Scattering-Zone Geometry in Meridian Plane.

be expected for field-aligned irregularities. An attempt was made to unveil any such effect by studying the "fine structure" of the upper-transit maximum with an averaging angle of less than one hour. No such effect was found on the basis of one year's Cygnus data. There were hints of such a magnetic effect in the data from both Cygnus and Cassiopeia when only six months' collections were used. The statistical variations in the data were comparable to the "hints", however, and the question must be considered open.

VI. CONCLUSIONS

A summary of the conclusions to be drawn from the work reported in this paper follows:

1) Radio-star visibility fades represent reductions in correlation of the star signals arriving at two interferometer antennas;
2) The reduced correlation results in at least a 50% (by definition) reduction in radio-star visibility for at least three minutes (by definition) and has been observed to reduce the visibility to zero for several minutes at a time and to last for up to considerably more than one hour;
3) Visibility fades in the auroral zone at sunspot maximum tend to occur at times of ionospheric transition (following the autumnal equinox, at magnetic midnight, during moderate cosmic-noise absorption and moderate magnetic disturbance, and possibly during the post-breakup phase of visual auroras);
4) Fades are caused by scattering irregularities whose latitudinal distribution peaks near the auroral maximum, and some of the same irregularities also act as inefficient backscatterers of HF radiation;
5) The scattering irregularities are distributed in height from at least as low as 100 kilometers to higher than 200 kilometers.

Regarding point (5), a speculation may be put forth that visibility fades require the simultaneous existence of irregularities in both the E-layer and the F-layer of the auroral ionosphere.

The above conclusions are based on observations at 223 MC with an interferometer of 91.44 meter (68.8λ) spacing.

VII. SUGGESTIONS FOR FURTHER WORK

Several questions have arisen out of the studies herein reported; among the most important are the following:

1) Are VHF visibility fades of radio stars representative of a normal condition in the auroral ionsophere or was the large occurrence of them during 1957-8 due to the sunspot maximum then under way, a maximum which apparently was itself an extreme one?
2) What is the cause of the autumnal maximum in fade occurrence, and is there a spring maximum or not?
3) What is the cause of the rather curious midafternoon peak in fade occurrence and of its apparent seasonal variation?
4) What is the latitudinal and height distribution of the fade-producing irregularities to a higher degree of precision than obtained in the present study? In particular, are two or more distinct layers of irregularities necessary for fade production?
5) What is the significance of the cases, noted during the present study, of fades occurring on 456 MC with no corresponding fade on 223 MC?

Several of the above questions require primarily theoretical studies for their answers, especially number (3) and the first question of number (2). On the other hand, number (5) probably requires additional experimental endeavor for its

answer. Answers to numbers (1) and (4) and to the second question of number (2) may possibly be found by further statistical analysis of existing data.

The following suggestions are made for further work which may answer some or all of the above questions:

1) routine scaling of existing interferometer records for periods other than sunspot max;
2) plotting of the annual distribution of fades from additional existing data, annual-distribution correlation studies with possibly related phenomena, theoretical investigation of question (2);
3) diurnal-distribution correlation studies with possibly related phenomena, theoretical investigation of question (3);
4) devising and testing of less restricted models for explanation of figure 12 of this report, plotting and interpretation of a similar figure for at least one full year of Cassiopeia data, plotting of additional data from both stars with narrower averaging angle, correction of height distribution for earth curvature;
5) operation of interferometers on several frequencies at the same location in the auroral zone.

An additional question is raised by observations at Saskatoon, published by Moorcroft and Forsyth (1963). They

report a stronger dependence of visibility-fade[1] occurrence on magnetic disturbance than that found in the present study. The question arises as to whether the discrepancy is due to a latitudinal effect or to a solar-cycle effect. The geomagnetic latitude difference between College and Saskatoon is only 4.1 degrees; the Saskatoon fades were observed between three and four years after the College fades which were analysed for this report. Analysis of later College data would clarify this point.

Aside from questions concerning visibility fades, another problem of the auroral ionosphere has emerged from the present study. Evidence of large-scale undulations in the ionosphere is apparent in the records. Occasional large enhancements of the radio-star signal, which appear on the records, may be caused by such "ionospheric lenses." An example of the enhancements found appears in figure 20. In the first few fringes at the left of the figure, there are several typical, slow, amplitude scintillations - most noticeable as enhancements. The fourth interference minimum is of reduced amplitude, possibly as a result of defocusing. In the center of the figure appears a particularly strong and lengthy enhancement which corresponds nearly to a three-db increase in star signal for almost three minutes.

---

[1] Moorcroft and Forsyth have used the term "radio star fadeout."

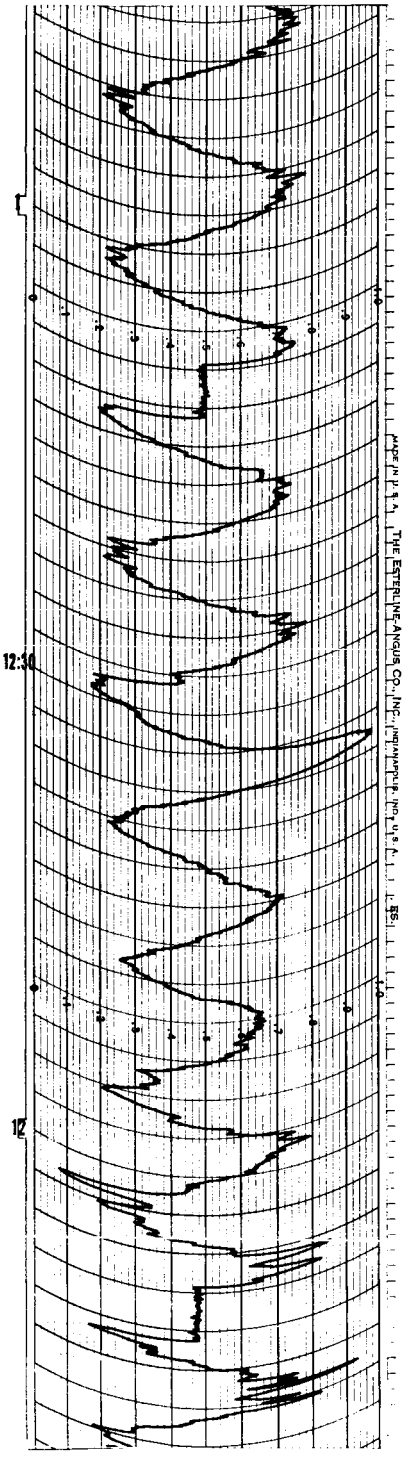

Fig. 20. Ionospheric Focusing Observed on Phase-Switch Interferometer.

Preliminary analysis of such ionospheric focusing and defocusing effects has been initiated at the Geophysical Institute (Owren, 1962b).

Much of the future work mentioned above will be carried out under an already approved extension of the present program. In particular, construction has begun of interferometers on 68 MC and 136 MC at the Ballaine Lake Field Site of the Geophysical Institute, where the 223 MC and 456 MC instruments used in the present studies are located. The new interferometers will include a capability for variation of baseline length, and the same feature will be added to the existing instruments. The variable-baseline interferometers will be able to "produce their own fades" by extension of baselines until the signal under track becomes uncorrelated. The technique is similar to that used in radio astronomy for measurement of angular diameters. The intended ionospheric application is to measure autocorrelation distance under a variety of radio-star seeing conditions.

APPENDIX I

Fortran Programs for Hour Angle and Coordinate Conversion

```
      IF (SENSE SWITCH 1)1,2
    1 READ 3,M,NO,DELTA,DA,T
    3 FORMAT (I9,I5,1X,F5.1,F5.0,F5.1)
      GO TO 4
    2 READ 5,M,DELTA,DA,T
    5 FORMAT (I9,6X,F5.1,F5.0,F5.1)
    4 GO TO (6,7,8,9,10,11,12,13,14,15,16,17),M
    6 P=0.
      GO TO 18
    7 P=31.
      GO TO 18
    8 P=59.
      GO TO 18
    9 P=90.
      GO TO 18
   10 P=120.
      GO TO 18
   11 P=151.
      GO TO 18
   12 P=181.
      GO TO 18
   13 P=212.
      GO TO 18
   14 P=243.
      GO TO 18
   15 P=273.
      GO TO 18
   16 P=304.
      GO TO 18
   17 P=334.
   18 Q=P+DA
      IF (DELTA-50.0)19,20,21
   19 D=201.
      GO TO 22
   21 D=253.
   20 CONTINUE
   22 CP=0.066*(D-Q)
      IF (CP)23,24,24
   23 C=24.0+CP
      GO TO 25
   24 C=CP
   25 HAP=T-C
      IF (HAP+12.0)34,34,35
   34 HA=24.0+HAP
      GO TO 38
   35 IF (12.0-HAP)36,36,37
   36 HA=24.0-HAP
      GO TO 38
```

```
37 HA=HAP
38 IF (SENSE SWITCH 1)26,27
26 PUNCH 28,M,NO,DELTA,HA
28 FORMAT (I3,I3,F5.1,F5.1)
   GO TO 1
27 K=DA
   IF (DELTA-50.0)29,30,31
29 TYPE 32,M,K,HA
32 FORMAT (I3,5H  CYG,I5,F7.1,4H HRS)
   GO TO 2
31 TYPE 33,M,K,HA
33 FORMAT (I3,5H  CAS,I5,F7.1,4H HRS)
30 GO TO 2
   END

   DIMENSION S(3),BETA(3),IRD(3)
   READ 1,S(1),S(2),S(3),BETA(1),BETA(2),BETA(3)
        IRD(1),IRD(2),IRD(3)
 1 FORMAT (F4.0,F5.0,F5.0,F5.0,F5.0,F5.0,I5,I5,I5)
10 READ 2,M,NO,DELTA,HA
 2 FORMAT (I3,I3,F5.1,F5.1)
   TYPE 11,M,NO,HA
11 FORMAT (/I3,I5,F7.1,4H HRS)
   XCOSZ=0.905*SIN(DELTA/57.3)+0.425*COS
        (DELTA/57.3)*COS(0.26*HA)
   XSINZ=SQRT(1.0-XCOSZ**2)
   XTANZ=XSINZ/XCOSZ
   XSINA=-COS(DELTA/57.3)*SIN(0.26*HA)/XSINZ
   XCOSA=SQRT(1.0-XSINA**2)
   H=110.
   DO 3 I=1,3
   DIMENSION E(3),B(3),D(3),R(3),THEAP(3),
        THETA(3),THEAD(3)
   IF (BETA(I))12,12,13
12 E(I)=H*XTANZ*XSINA
   B(I)=S(I)+H*XTANZ*XCOSA
   GO TO 14
13 E(I)=S(I)*SIN(BETA(I)/57.3)+H*XTANZ*XSINA
   B(I)=S(I)*COS(BETA(I)/57.3)+H*XTANZ*XCOSA
14 D(I)=SQRT(E(I)**2+B(I)**2)
   R(I)=SQRT(D(I)**2+H**2)
   IF (R(I)-300.)3,4,4
 4 IF (1200.-R(I))3,6,6
 6 THETA(I)=ATAN(E(I)/B(I))
   THEAP(I)=THETA(I)-28.0/57.3
   IF (COS(THEAP(I))-0.866)3,16,16
16 IF (THEAP(I)-3.1)7,7,8
 7 THEAD(I)=57.3*THEAP(I)
   GO TO 15
 8 THEAD(I)=-(360.0-57.3*THEAP(I))
```

```
15 TYPE 9, IRD(I), THEAD(I),R(I)
 9 FORMAT (12HRADAR NUMBER,I3,F6.0,4H DEG,F7.0,
       3H KM)
 3 CONTINUE
   GO TO 10
   END
```

APPENDIX II

Fortran Program for Compiling of Riometer Data

```
      DIMENSION N(201),K(11),L(201)
      N(1)=0
      DO 1 I=2, 201
    1 N(I)=N(I-1)
    2 READ 3,K(1),K(2),K(3),K(4),K(5),K(6),K(7),K(8),
     1    K(9),K(10),K(11)
    3 FORMAT (I3,I3,I3,I3,I3,I3,I3,I3,I3,I3,I3)
      DO 4 J=1,10,3
      DO 4 I-1,201
      IF (K(J)-I-1)4,5,4
    5 N(I)=N(I)+1
    4 CONTINUE
      IF (SENSE SWITCH 1)8,2
    8 M=10
      TYPE 6,M
    6 FORMAT (11HABS. IN DBX,13,23H          NO. OF
     1    OCCURRENCES)
      DO 9 I=1,201
      L(I)=I-1
    9 TYPE 7,L(I),N(I)
    7 FORMAT (I8,I16)
      END
```

REFERENCES

Benson, R. F., Effect of Line-of-sight Aurora on Radio Star Scintillations, J. Geophys. Res., 65, 1981, 1960.

Bolton, J. G., Slee, O. B., and Stanley, G. J., Galactic Radiation at Radio Frequencies. VI. Low Altitude Scintillation of the Discrete Sources, Australian J. Phys. A, 6, 434-451, 1953.

Bolton, J. G., and Stanley, G. J., Variable Source of Radio Frequency Radiation in the Constellation of Cygnus, Nature, 161, 312-313, 1948.

Booker, H. G., The Use of Radio Stars to Study Irregular Refraction of Radio Waves in the Ionosphere, Proc. IRE, 46, 298-314, 1958.

Booker, H. G., Ratcliffe, J. A., and Shinn, D. H., Diffraction from an Irregular Screen with Applications to Ionospheric Problems, Phil. Trans. Roy. Soc. A, 242, 579-607, 1950.

Born, M., and Wolf, E., Principles of Optics, Pergamon Press, New York, 1959.

Davis, T. N., An Investigation of the Morphology of the Auroral Displays of 1957-8 (Doctoral disertation), University of Alaska, 1961.

Fejer, J. A., The Diffraction of Waves in Passing through an Irregular Refracting Medium, Proc. Roy. Soc. A, 220, 455-471, 1953.

Flood, private communication to L. Owren, 1962.

Hewish, A., The Diffraction of Radio Waves in Passing through a Phase-changing Ionosphere, Proc. Roy. Soc. A, 209, 81-96, 1951.

Hey, J. S., Parsons, S. J., and Phillips, J. W., Fluctuations in Cosmic Radiation at Radio Frequencies, Nature, 158, 234, 1946.

Leonard, R. S., Distribution of Radar Auroras over Alaska (Doctoral disertation), University of Alaska, 1961.

Little, C. G., Merritt, R. P., Stiltner, E., Cognard, R., Radio Properties of the Auroral Ionosphere (Quarterly progress report no. 6), Geophysical Institute of the University of Alaska, 1957.

Little, C. G., Rayton, W. M., Roof, R. B., Review of Ionospheric Effects at VHF and UHF, Proc. IRE, 44, 992-1018, 1956.

Little, C. G., Reid, G. C., Stiltner, E., Merritt, R. P., An Experimental Investigation of the Scintillation of Radio Stars Observed at Frequencies of 223 and 456 Megacycles per Second from a Location Close to the Auroral Zone, J. Geophys. Res., 67, 1763-1784, 1962.

McCready, L. L., Pawsey, J. L., Payne-Scott, R., Solar Radiation at Radio Frequencies and its Relation to Sunspots, Proc. Roy. Soc. A, 190, 357-375, 1947.

Moorcroft, D. R., Radio Star Fadeouts on Phase-Switching Interferometer Records, J. Geophys. Res., 68, 111-115, 1963.

Moorcroft, D. R., and Forsyth, P. A., On the Relation Between Radio Star Scintillations and Auroral and Magnetic Activity, J. Geophys. Res., 68, 117-124, 1963.

Nichols, private communication to L. Owren, 1960.

Owren, L., Radio Properties of the Auroral Ionosphere (Final Report, Part 1), Geophysical Institute of the University of Alaska, 1962.

Owren, L., private communication, 1962.

Ratcliffe, J. A., Some Aspects of Diffraction Theory and their Application to the Ionosphere, Rep. Prog. Phys., 19, 188-267, 1956.

Smith, F. G., Little, C. G., and Lovell, A.C.B., Origin of the Fluctuations in the Intensity of Radio Waves from Galactic Sources, Nature, 165, 422-424, 1950.

Starr, A. T., Radio and Radar Technique, Pitman and Sons, London, 1952.

Tryon, H. M., Auroral Index for College, Alaska, Derived from All-Sky Camera Photographs (Scientific Report No. 2), Geophysical Institute of the University of Alaska, 1959.